UCONN LIBRARY

University of Connecticut
OpenCommons@UConn

Master's Theses | University of Connecticut Graduate School

7-5-2012

Three-Dimensional Force Systems Produced by Vertical V-Bends in an Arch Wire

Raja Shah
University of Connecticut School of Medicine and Dentistry, rashah@gde.uchc.edu

Recommended Citation
Shah, Raja, "Three-Dimensional Force Systems Produced by Vertical V-Bends in an Arch Wire" (2012). *Master's Theses*. 301.
https://opencommons.uconn.edu/gs_theses/301

This work is brought to you for free and open access by the University of Connecticut Graduate School at OpenCommons@UConn. It has been accepted for inclusion in Master's Theses by an authorized administrator of OpenCommons@UConn. For more information, please contact opencommons@uconn.edu.

Three-Dimensional Force Systems Produced by Vertical V-Bends in an Arch Wire

Raja Abhilash Shah

B.S., University of New Mexico, 2006
D.D.S., University of the Pacific, 2009

A Thesis

Submitted in Partial Fulfillment of the

Requirements for the Degree of

Master of Dental Science

at the

University of Connecticut

2012

APPROVAL PAGE

Master of Dental Science Thesis

Three-Dimensional Force Systems Produced by Vertical V-Bends in an Arch Wire

Presented by

Raja Abhilash Shah, B.S., D.D.S.

Major Advisor _____
Ravindra Nanda, B.D.S., M.D.S., Ph.D.

Associate Advisor _____
Flavio A. Uribe, D.D.S., M.D.S

Associate Advisor _____
Madhur Upadhyay, B.D.S., M.D.S., M.Dent.Sc.

Associate Advisor _____
Donald R. Peterson, B.S., M.S., Ph.D.

University of Connecticut

2012

Acknowledgements:

I would like to express my sincere gratitude to my major advisor, Dr. Ravindra Nanda, and my associate advisors, Dr. Flavio Uribe, Dr. Madhur Upadhyay, and Dr. Donald Peterson, for their guidance and encouragement throughout this project. A special thanks to Takafumi Asaki for his role in building the testing apparatus and writing the associated software. I would like to thank Orlando Sarria at Ultimate Wireforms, Inc. for providing all of the wires used in this study and American Orthodontics for providing the brackets.

Thank you to all of the faculty, residents, and staff at the University of Connecticut, Division of Orthodontics with whom I have had the absolute pleasure of working for the last three years. I am very grateful for the time I have spent at UConn and for the opportunity to study orthodontics here.

Table of Contents

Introduction:

An important aspect of clinical orthodontic treatment is the knowledge of the force systems produced when various appliances are used. A clear understanding of biomechanical principles can help the clinician produce more predictable results and minimize potential side effects of a specific orthodontic setup. (1) Although the force systems can become quite complex when multiple teeth are considered, a helpful starting point can involve a simple two-bracket system. The orthodontic literature includes a detailed two-dimensional analysis of the force systems produced when a straight wire is engaged into two nonaligned brackets. By simply examining the angle each bracket makes relative to the line connecting the two brackets, the orthodontist can determine the relative force system. This relative force system consists of the directions and ratio of the moments in the same plane of the brackets, as well as the directions of the vertical forces at both brackets. (1) A similar analysis can be applied to a two-bracket system that consists of a wire with a vertical v-bend engaged into two aligned brackets. By measuring the distance of the v-bend from one bracket relative to the distance between the brackets, the relative force systems can again be determined. (2) Although these studies provide a basis for understanding the biomechanical principles, certain limitations must be considered when attempting to apply them to a clinical situation. For example, the force systems were not observed experimentally. Instead, they were calculated using a mathematical model which included several assumptions regarding the properties and behavior of the wire. One such assumption was that the wire was completely free to slide within the brackets, and thus, any effects of friction and mesiodistal forces were ignored. To avoid these types of assumptions and to more closely simulate a clinical situation, an

in-vitro study was conducted to examine the effects of varying the mesiodistal position of a vertical v-bend in a wire engaged into two aligned brackets. However, this study only reported on the moments generated within the plane of the brackets. (3) It is important to note that all of the studies mentioned above involved a symmetrical two-bracket system with two identical brackets in one plane of space. The only forces considered were those in a vertical direction, and the only moments discussed were those created by a second-order deflection of the wire within the brackets (mesial or distal tip of the tooth). Thus, these studies were limited to a partial two-dimensional analysis of the force systems produced. In order to account for the curvature of a dental arch and arch wire, a study examining the effect of a vertical v-bend in a three-dimensional two-bracket system was conducted. This study involved the right half of the maxillary arch simulated using a finite element model, so certain assumptions regarding the wire properties were necessary to run this computer based analysis. The two brackets were asymmetric in their orientation and position around the dental arch since they simulated the brackets at the first molar and the central incisor. Here, the moments of interest were those that are caused by a second-order deflection at the molar bracket (mesial or distal tip) and a third-order deflection at the incisor bracket (facial or lingual tip). (4) Although this was a three-dimensional setup, the authors only reported on the vertical forces at each bracket and on the moments mentioned above, which were oriented only in the sagittal plane. Therefore, the rationale for the current study was to provide a more thorough three-dimensional analysis of the force systems produced by varying the position of a vertical v-bend in an arch wire. This was accomplished using an in-vitro setup simulating a maxillary dental arch. Both the left and right central incisor and first molar brackets were

oriented in their proper positions around the dental arch, and full arch wires with incorporated v-bends were engaged into these brackets. In order to provide a more complete three-dimensional understanding of the force systems produced, the forces and moments in all three planes of space at both a molar and incisor bracket were recorded and analyzed.

Background:

Force Systems in Orthodontics

Orthodontic tooth movement is a result of the force system applied to the teeth. (5; 6) Force systems consist of the applied forces as well as the rotational components, or moments. A force may be represented as a vector, which must describe the magnitude, direction, and point of application of the force. (6; 7) A force acting on a tooth will produce different movements depending on the relationship among the line of action and point of application of the force and the center of resistance (CR) of the tooth. The CR is defined as the point at which a force through it will result in translation of the tooth along the line of action with no rotation, and its position varies with factors such as root length and alveolar bone height. (7) A force acting on tooth at any point other than the CR will result in a translatory force as well as a rotational component called the moment of the force; it is calculated by multiplying the magnitude of the force by the perpendicular distance of the line of action to the CR, and its direction is found by following the line of action around the CR. (5; 6) Finally, a pure rotational movement, defined as a tooth spinning about its CR, is produced by a moment of a couple. (7) A couple is comprised of two forces of equal magnitude with parallel lines of action but in opposite directions and separated by a distance (non-collinear). (5) The magnitude of the moment is calculated by multiplying the magnitude of one of the forces by the distance between them, and the direction is found by following one force to the origin of the other force. Such a system will produce rotation about the CR regardless of where on the object the couple is applied. (5; 6) An understanding of the force systems delivered from

commonly used orthodontic appliances may result in more predictable tooth movement with fewer side effects. (1)

Two-Bracket Geometries

When an arch wire is placed in a set of brackets in the mouth, a complex force system is produced along the arch. To aid in understanding this force system, it is helpful to simplify it into a series of two-tooth segments which can then be summed to estimate the force system at each tooth. Utilizing the laws of statics, Burstone and Koenig describe in detail the initial force system produced by placing a wire into two nonaligned brackets. Based on the fact that the wire is in equilibrium, the forces and moments acting on it (activation force system) can be reversed to show the forces and moments acting on the teeth (deactivation force system). To simplify the descriptions of the force systems, Burstone and Koenig considered only one plane of space (two dimensions) and disregarded the effects within the bracket slots. To begin determining the force system, one must first identify the interbracket axis (L), which is the line connecting the centers of the two brackets. Next, Θ_A and Θ_B are measured as the angles formed by the brackets with respect to L (Figure 1). (1)

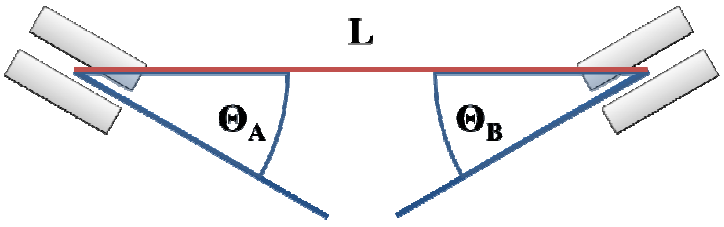

Figure 1

Burstone and Koenig present six basic two-bracket geometries, which are defined by the ratio of Θ_A/Θ_B. A Class I geometry is the configuration when both brackets form

the same angle in the same direction with respect to L. A Class II geometry occurs when both angles are in the same direction, but one angle measures half of the other angle. A Class III geometry involves the situation in which one of the brackets is parallel to L, which results in $\Theta_A/\Theta_B = 0$. Class IV, V, and VI describe configurations in which both brackets form angles in opposite directions with respect to L. In a Class IV geometry, one angle is half that of the other; in a Class V geometry, one angle is ¾ that of the other; and in a Class VI geometry, both angles are equal in magnitude. Each of these geometries depends only on the angles of the brackets to the interbracket axis, and they represent a relative force system that does not vary despite changes in such factors as interbracket distance and amount of activation. In other words, for each of the geometries, the directions and ratio of the moments (M_A/M_B) produced remains constant. In addition to the moments, each geometry produces a vertical force at each bracket. The magnitudes of both of these forces are always equal to one another, and their directions are always opposite to one another. In general, if all other factors are held constant, the magnitude of the forces is highest at a Class I geometry, and it decreases moving toward a Class VI geometry, where the forces are equal to zero. Table 1 describes the specific force systems for each of the six geometries. (1)

	Θ_A/Θ_B	M_A/M_B	Force System
Class I	1.0	1.0	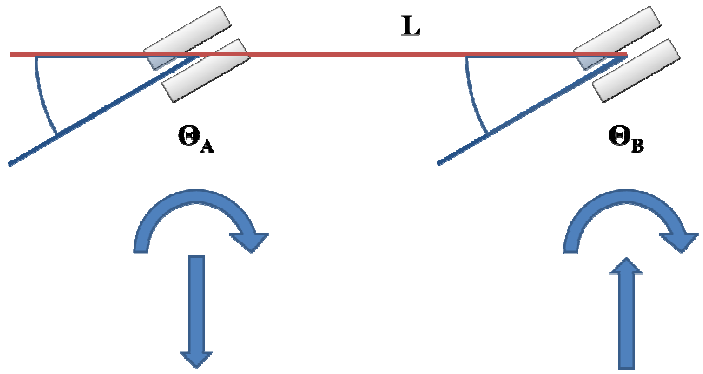
Class II	0.5	0.8	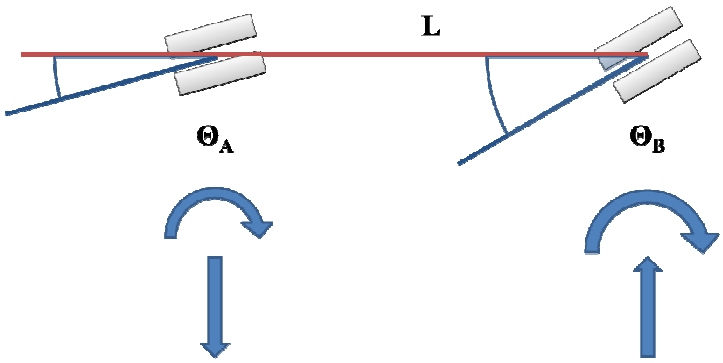
Class III	0	0.5	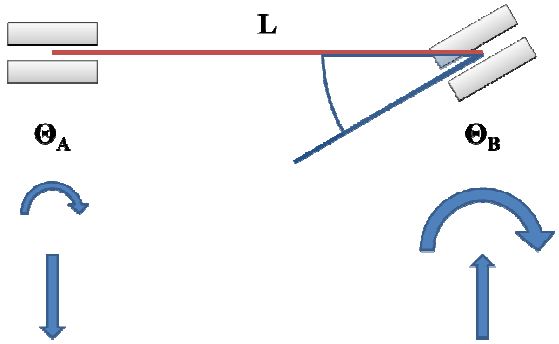
Class IV	-0.5	0	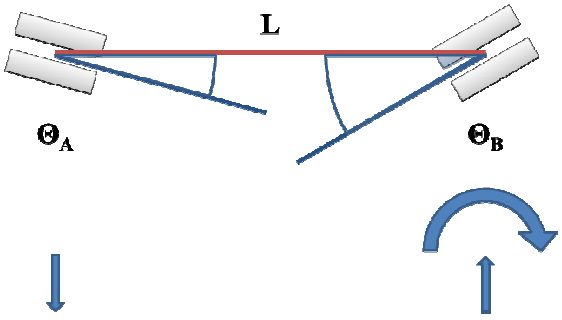

Class V	-0.75	-0.4	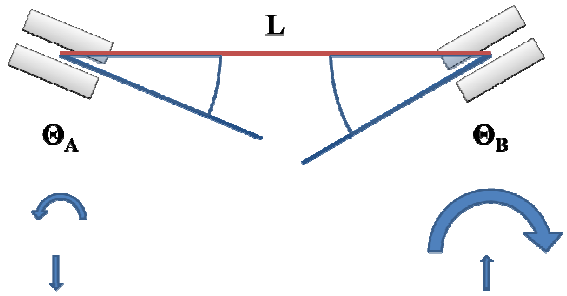
Class VI	-1.0	-1.0	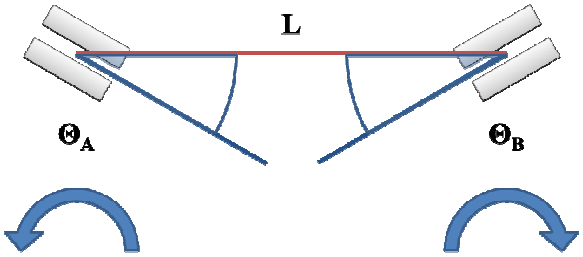

Table 1

It is important to observe that the six geometries are representative of a continuum of possible configurations and force systems between two brackets. Therefore, in a clinical setting, the orthodontist can estimate which geometry applies and determine the direction of the moments, their relative magnitudes, and direction of the vertical forces. This information can be quite useful even without knowing the exact magnitudes. Note that these two-bracket geometries only give the initial force system acting on the teeth, and that it will change as the wire deactivates and the teeth move. However, the initial force system is nonetheless significant in that it is the force system with the greatest magnitude and the one most likely to be applicable while the wire is engaged in the brackets. In addition, the force systems given are those acting at the brackets. In order to determine how a tooth may move, one must consider the moment to force ratio at the attachment and replace it with the equivalent force system at the CR of the tooth or group of teeth. (1)

Step Bends and V-Bends

Burstone and Koenig have shown how placing a straight wire into two malaligned brackets can produce predictable force systems based on the angles formed between the brackets and the interbracket axis. (1) Similarly, it has been shown how placing a bend in a wire between two brackets can also produce predictable force systems. (2; 8) Burstone and Koenig studied the force systems created by two commonly used bends: the step bend and the V-bend. The moments and forces in one plane were calculated mathematically using an analytical model with the important assumption that the wire has full freedom to slide, and therefore, there are no mesiodistal forces. When engaging a wire with a step bend between the two brackets, the brackets will experience vertical forces with equal magnitudes but opposite directions, as well as moments with equal magnitudes and the same directions (Figure 2).

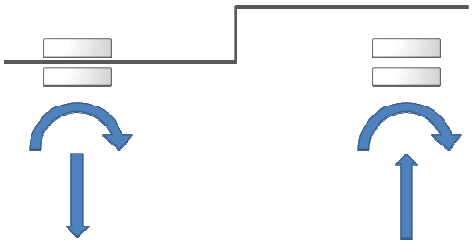

Figure 2

This force system is identical to that produced by a straight wire engaged into two parallel stepped brackets (Class I geometry). In general, varying the position of the step bend mesiodistally between the two brackets does not change the absolute or relative force system. Increasing the height of the step increases the magnitudes of the moments linearly, but the relative force system does not change, meaning the ratio of the moments is always $M_A/M_B = 1$. This ratio is also independent of the interbracket distance,

although the magnitudes of the forces and moments decrease as interbracket distance increases. (2)

If a V-bend is placed between two brackets, the mesiodistal position of the bend is very important in determining the resulting force system. (2; 8) The position of the apex of the V-bend can be described by the a/L ratio, where a is the distance of the bend from one bracket and L is the interbracket distance (Figure 3).

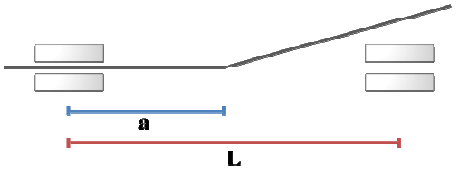

Figure 3

Thus, a continuum of force systems can be portrayed based on a/L. If the V-bend is centered between the brackets (a/L = 0.5), then the moments at each bracket, M_A and M_B, will be equal and in opposite directions ($M_A/M_B = -1$). (2) This force system corresponds to that of a Class VI geometry. (8) If the V-bend is one third of the distance from bracket A (a/L = 0.33), then there is only a force at bracket B and no moment. (2) This specific position for the bend is called the point of dissociation, and this force system is identical to that of a Class IV geometry. (8) Finally, as the bend is moved increasingly toward bracket A, the moments at both brackets will be in the same direction with the larger moment at bracket A. (2) With a V-bend in this extreme third of the interbracket distance, the force system begins to approximate that of a Class III geometry. (8) These specific examples are shown in Figure 4.

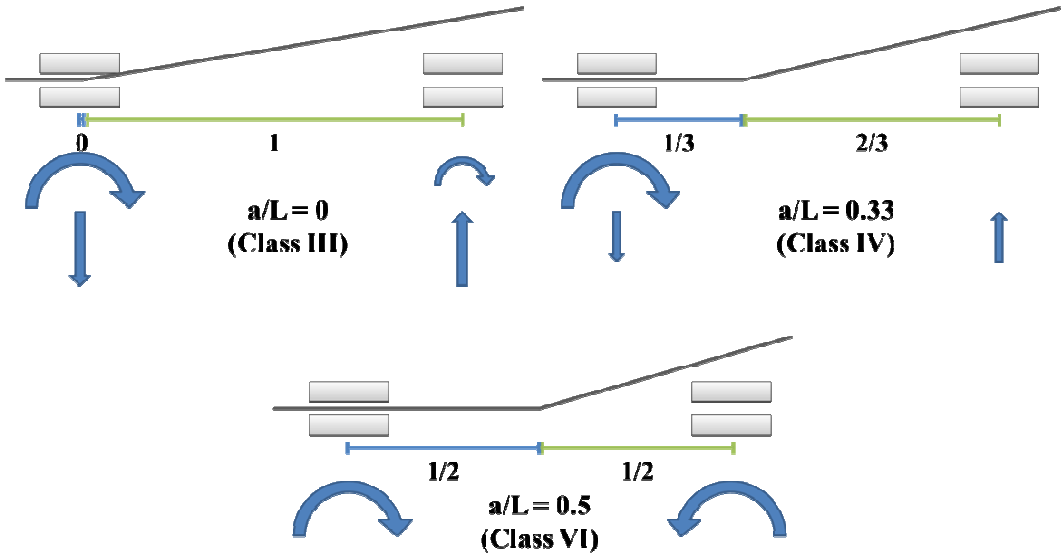

Figure 4

The forces produced are also affected by the a/L ratio; as one moves the bend farther from the center towards either bracket, the vertical forces increase nonlinearly from zero. As in step bends, the magnitudes of the forces and moments decrease with increasing interbracket distance, but the ratio of the moments remains constant. Clinically, the interbracket distance can play a significant role in the resulting force system. For example, when the interbracket distance is 7 mm, an error of 1 mm in the position of the V-bend can be enough to change the directions of the moments, whereas the same error when the interbracket distance is 14 mm may not significantly change the relative force system. Finally, increasing the height of the V-bend does not alter the relative force system (M_A/M_B), but the magnitudes of the moments and forces do increase. (2) It is important to note that this relationship is true only if the bend is not so great that the activation results in permanent deformation of the wire (must remain within the elastic limit). (2; 8) To control the exact magnitudes of the moments and forces, one must consider the interbracket distance, the wire material and size, and the V-bend size and

position. (8) However, in a clinical setting, an understanding of these basic relationships can aide in applying the correct relative force system.

Nickel-Titanium Wires

Nickel-titanium (NiTi) alloys are quite useful in orthodontics due to their specific characteristics known as superelasticity and shape memory. Superelasticity results from the fact that NiTi can exist in two distinct crystallographic phases: martensite and austenite. In the martensitic phase, the three-dimensional lattice of atoms is body-centered, while in the austenitic phase, it is face-centered. The transformation between these two phases, or reorganization of the crystal structure, is reversible; in most other metals and alloys, the same amount of stress would cause permanent deformation. The specific temperature range in which this phase change occurs is called the temperature transitional range (TTR). (9) This range is depicted graphically in Figure 5.

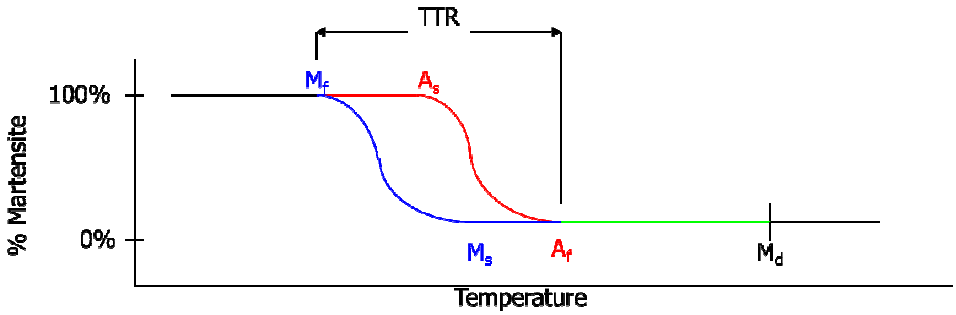

Figure 5 (10)

A_s and A_f are the temperatures at which the austenite phase starts and finishes forming, respectively. Similarly, M_s and M_f are the temperatures at which the martensite phase starts and finishes forming, respectively. At low temperatures, the alloy exists completely in the martensitic phase until the temperature is increased to A_s, when the austenitic phase begins to form. As it is further increased to A_f and beyond, the alloy

exists completely in the austenitic phase. The reverse transformation occurs as the temperature is decreased from M_s to M_f. This property of NiTi is referred to as thermoelasticity and gives rise to its shape memory effect. During fabrication involving deflection and temperature cycles, the wire is able to "memorize" a preformed shape, such as a dental arch form, in the austenitic phase. When the temperature is decreased, the wire is in the martensitic phase and is pliable and easily deformed. However, when the temperature increases and it is converted into the austenitic phase, the wire will recover to the preformed shape. (9) In general, the austenitic phase of a NiTi alloy is stiffer than the martensitic phase. (9; 11) NiTi alloys with TTRs between room and body temperature are termed martensitic active, are pliable in and out of the mouth, deliver low forces, and will not convert into the stiffer austenitic phase unless the temperature increases beyond 40ºC. NiTi alloys with TTRs below room temperature are already in the austenitic phase at room temperature and remain so intraorally. NiTi alloys with TTRs near body temperature are in the soft martensitic phase outside the mouth, but they are activated and spring back to their original shape at body temperature. (9) When NiTi is completely transformed into austenite, it exhibits a characteristic "superelastic plateau" in the stress-strain curve, which can be seen in Figure 6. (9; 11)

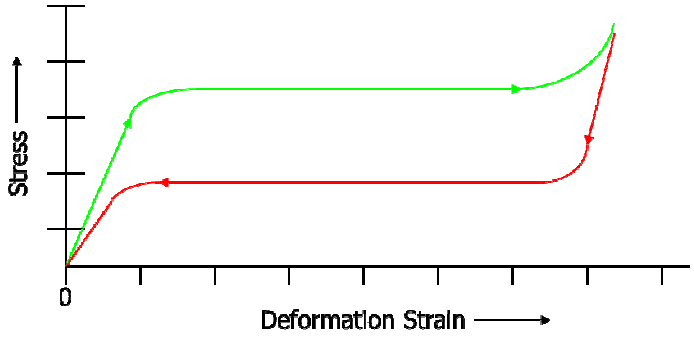

Figure 6 (10)

In the initial segment of the curve, before significant deformation has taken place, NiTi behaves similar to other alloys, such as stainless steel, in that the stress and strain are directly proportional. In this region, the alloy is stiff and not exhibiting its superelastic properties. The next segment is the superelastic plateau and it is specifically due to the pseudoelastic properties of NiTi. Pseudoelasticity is caused by a local transformation from austenite to martensite due to a local increase in stress. This phenomenon is called stress-induced martensite (SIM), and SIM only forms in areas of stress while the rest of the wire remains austenitic. The SIM is unstable and will revert to austenite as soon as the stress is removed. (9; 11) Once the SIM is formed, the horizontal portion of the curve begins. Here, the NiTi "absorbs" any additional stress and remains flat. The upper curve represents activation, or the force required to activate the wire, and the lower curve represents deactivation, or the force delivered to the teeth. This tendency is termed hysteresis. These traits are clinically important because as one gradually increases the deflection in a wire (before permanent deformation) the activation force required is constant, and the force released from the wire is also constant but at a lower level. (11) In conclusion, NiTi alloys demonstrate superelastic properties because of their thermoelasticity (phase change along a TTR) and their pseudoelasticity (localized formation of SIM). (9)

Beta Titanium Wires

Another popular class of wires known as beta titanium alloys was introduced for orthodontic use by Burstone and Goldberg. (12; 13; 14) At very high temperatures (above 885ºC), pure titanium rearranges its crystal structure into a body-centered cubic

lattice known as the beta phase. However, with the addition of other elements like molybdenum, the beta phase can exist at room temperature, and these beta-stabilized titanium alloys have a unique set of properties. (12) Previously, stainless steel was the primary orthodontic alloy. (13) For a set cross section, beta titanium can be deflected approximately twice as much as steel without permanent deformation. (12; 15) The modulus of elasticity (a measure of stiffness) of beta titanium is less than half of that of steel and about twice that of nitinol (an early nickel titanium alloy). (12; 13; 15) This can be readily seen in the linear portion of a load-deflection graph comparing the materials (Figure 7). The stiffness is related to the slope of each curve, and it is clear that solid stainless steel has the highest stiffness, followed by beta titanium (BIII-CNA), and then NiTi (Black-Ti SE, Superelastic I, and Ultra Therm wires).

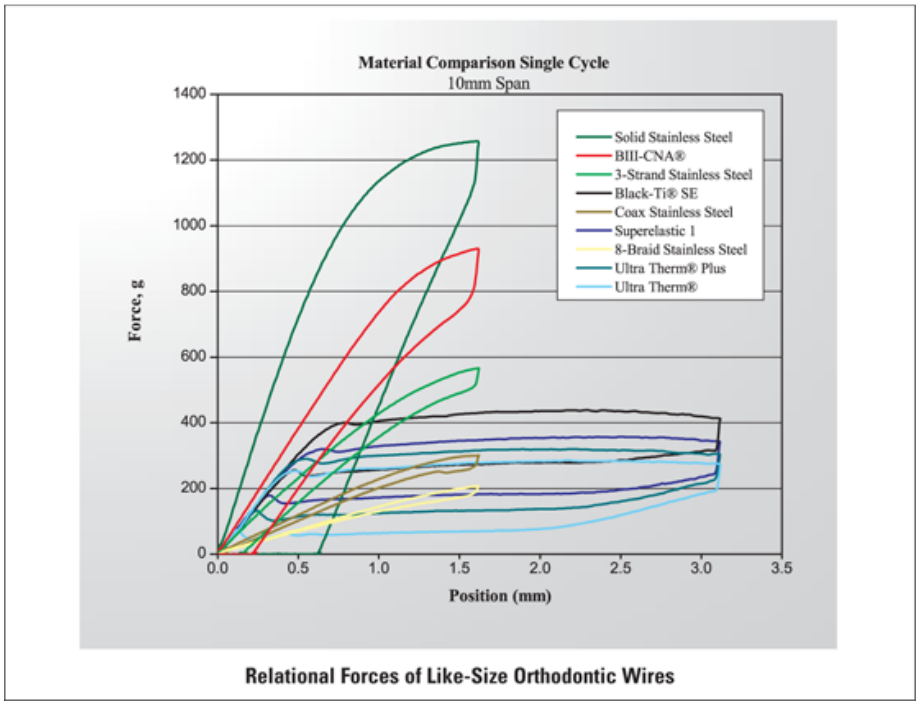

Figure 7 (16)

In addition to delivering lower forces than stainless steel, beta titanium has a higher springback (extent of recovery upon deactivation of an activated wire), and it can accept

bends. (12; 14) Thus, its properties make beta titanium a needed step between soft, unadjustable NiTi and very stiff, formable stainless steel. (13) Clinically, beta titanium is valuable because the unwanted side effects produced from a beta titanium wire can be counteracted with lower forces than those needed to counteract side effects from a similar steel wire. In addition, loops and helices are often needed with steel wires to reduce the load deflection rate, but these may be unnecessary with beta titanium wires again due to the low stiffness and high springback. (15) Despite these favorable traits, beta titanium has a potential flaw because the coefficient of friction is higher than most other orthodontic alloys, which may hinder sliding mechanics in the mouth. (14; 15) Therefore, a new beta titanium alloy known as CNA was introduced into the market. This alloy was a modification on the existing beta titanium wires to improve the surface characteristics and exhibit a smooth, high-polish finish. (10) An experimental study examining surface roughness and friction among different beta titanium alloys by Kusy et al. confirmed that CNA had the smoothest surface, and they found that the coefficients of friction were second lowest of the five beta titanium alloys tested. (17)

V-Bends in NiTi and Beta Titanium Wires

Quick et al. conducted an in vitro study to examine the effect of V-bend positioning in NiTi and TMA wires. They used 0.018" × 0.025" and 0.016" × 0.022" NiTi wires and 0.017" × 0.025" and 0.016" × 0.022" inch TMA wires. V-bends included angles of 135, 150, and 165 degrees, and these bends were positioned along the interbracket distance in 1 mm increments. The setup consisted of two aligned lower incisor brackets with zero tip and torque, the moment was measured at one bracket with a

transducer, and the temperature was controlled at 36.0 ± 0.5°C. Overall, the moment increased as the V-bend approached the transducer. For TMA, this trend was linear, which was consistent with patterns seen in previous studies. For most of the NiTi wires, the curves were initially linear, but then tended to flatten as the bend approached the transducer. A possible explanation for this finding could be that as the bend approached the transducer, the increased stress caused the formation of SIM and the wire to exhibit superelastic behavior. Only the 0.018" × 0.025" NiTi with the 165 degree bend exhibited a linear graph; this was likely because the large cross-sectional area and the shallow angle combined may not have let SIM to form. Another major difference between the two wire materials was the point of dissociation. For all the TMA wires combined, the point of dissociation was shown to be at an interbracket ratio of 0.27. This is similar to the results by Burstone and Koenig, who calculated this point to be at an interbracket ratio of 0.33. However, for NiTi wires, this point was calculated to be at an interbracket ratio of 0.033, which is almost immediately adjacent to one of the brackets. Thus, a V-bend in a NiTi wire in a two bracket geometry will usually produce two moments in opposite directions regardless of the position of the bend. The exception is when the bend is next to one of the brackets, in which the moment at the opposite bracket will approach zero. (3)

3-Dimensional (3D) Analysis of Force Systems

Until recently, most analyses of orthodontic force systems have been in 2-dimensions (2D). These studies include describing the forces and moments produced by a V-bend placed between two collinear brackets or a straight wire placed between two noncollinear brackets, and these force systems were limited to one plane of space. To

simulate a 3D configuration, Isaacson et al. developed a finite element study simulating a 2x2 appliance in which a wire is inserted only into the maxillary first molar and central incisor brackets. Only the right half of the arch was modeled, and a global coordinate system was applied to the teeth. A 0.017" × 0.025" stainless steel arch wire with single vertical V-bends introduced at different locations along the interbracket distance was simulated. This study only reported the moments that would cause a second order (mesiodistal) rotation in the molar and a third order (facial-lingual) rotation in the incisor. The forces that were included were the associated equilibrium forces at each tooth, which were the intrusive or extrusive vertical forces. The position of the V-bend was defined by the a/L ratio, where a was the distance from the molar bracket to the bend, and L was the total interbracket distance. Both measurements were taken along the arch wire perimeter. The wire was assumed to be fully elastic for all activations. The results showed that the 3D force systems are not symmetrical nor centered around the point where a/L = 0.5 as they are in 2D systems. The authors found that at a/L = 0.45 (slightly off-center towards the molar) is where a V-bend will produce equal and opposite moments at the molar and incisor brackets, and the forces will be zero. As the V-bend moves toward the molar, the distal tip moment at the molar increases and the facial torque moment at the incisor decreases. This moment at the incisor does not reach zero (point of dissociation) and reverse its direction until the a/L ratio is reduced to 0.14. This finding differs from the 2D system where the point of dissociation is at a/L=0.33. Moving the V-bend from the center towards the incisor results in a progressively decreasing distal tip moment at the molar and an increasing facial torque moment at the incisor. Here, the point of dissociation is at 0.63, which is where the moment at the molar becomes zero, and as the

V-bend continues to move toward the incisor, the moment at the molar is reversed to a mesial tip moment and progressively increases. This finding is similar to a 2D system where the point of dissociation occurs when the V-bend is twice as far from one bracket as the other (a/L=0.67). As the V-bend progresses from a/L=0.45 towards the molar, an extrusive force at the molar and an intrusive force at the incisor gradually increase. Conversely, as the V-bend progresses from a/L=0.45 towards the incisor, an intrusive force at the molar and an extrusive force at the incisor gradually increase. This study has effectively shown that when placing a V-bend in a 3D asymmetrical system (molar and incisor around a curve) instead of a 2D symmetrical system (2 identical brackets in one plane), a different force system is produced that cannot be extrapolated from a 2D projection onto the curved arch wire. The authors suggest the reason for this difference is that a 3D rectangular arch wire experiences torsion when activated in 2x2 appliance, and this torsion progressively increase as the V-bend is moved toward the incisor. Since this torsion provides extra resistance to the deformation in the anterior leg of the wire, the neutral point where the moments are equal and opposite becomes located slightly more posteriorly. (4) Although the data from this study incorporated 3D arch wires, all 3D aspects were not considered. The molar and incisor were in different planes of space, but the measured force system at each tooth individually was only in one plane. The moments reported were around only 1 axis, and the forces were only in the intrusive/extrusive direction. Unfortunately, there are a small number of studies in which computer modeling is used to determine 3D force systems. (18) There are even fewer studies in which 3D experimental measurements are used and all six components of the force system (forces along all 3 axes and moments around all three axes) are analyzed.

Such studies in the recent literature involve the force systems produced from T-loop arch wires (19) and from a high canine malocclusion. (18; 20; 21)

Objectives:

1. To experimentally determine the 3D force systems produced by vertical V-bends placed at different locations along the interbracket distance in a rectangular arch wire engaged in a 2x2 appliance.
2. To compare the force systems produced by arch wires of different materials (NiTi and CNA).
3. To compare the force systems produced by arch wires of different dimensions (0.016" x 0.022", 0.017" x 0.025", and 0.021" x 0.025").

Hypotheses:

1. The force systems produced by vertical V-bends in a rectangular arch wire will consist of significant forces and moments in all 3 dimensions at the maxillary first molar and central incisor brackets in a 2x2 appliance, and these force systems will vary based on the position of the V-bend.
2. There will be no significant difference in the force systems produced by NiTi and CNA arch wires. (null hypothesis)
3. There will be no significant difference in the force systems produced by wires of different dimensions. (null hypothesis)

Materials and Methods:

Setup

Before beginning to perform experiments with the individual arch wire samples, a testing apparatus was constructed. The major components of the apparatus included a series of aluminum pegs arranged to represent the teeth in a maxillary dental arch. In addition, two of the pegs (those representing the right central incisor and right first molar) were connected to sensors which have the ability to measure forces and moments in three dimensions: F_x, F_y, and F_z; and M_x, M_y, and M_z. These sensors were ATI NANO 17 SI-50-0.5 F/T sensors, and the characteristics given by the manufacturer are shown in Table 2.

	Range	**Resolution**
F_x, F_y	5,100 g	1.275 g
F_z	7,140 g	1.275 g
M_x, M_y	51,000 g·mm	6.375 g.mm
M_z	51,000 g·mm	6.375 g.mm

Table 2

The twelve pegs, representing the maxillary teeth up to the first molars, were arranged in the shape of a dental arch using a predefined arch form, OrthoForm III – Ovoid from 3M Unitek. The pegs were positioned along the arch such that when brackets are adhered to them, the bracket slots would follow the arch form. The distances between the pegs were calculated using average tooth widths. Once the pegs were secured to an aluminum plate, a set of self-ligating brackets, Empower series from American Orthodontics, were bonded

to both central incisor pegs using a composite resin, and both first molar pegs were bonded with single tubes. The slot dimension for all teeth was 0.022" x 0.028". A full dimension stainless steel wire was used as a jig to align the brackets and ensure that they were bonded in a neutral position, meaning they would express zero tip and zero torque. Theoretically, any arch wire in the specific shape of OrthoForm III should lie passively when engaged into the brackets. Finally, the sensors were connected to a computer to record the readings, and the entire apparatus was placed in an enclosed chamber. A diagram of the apparatus is shown in Figure 8.

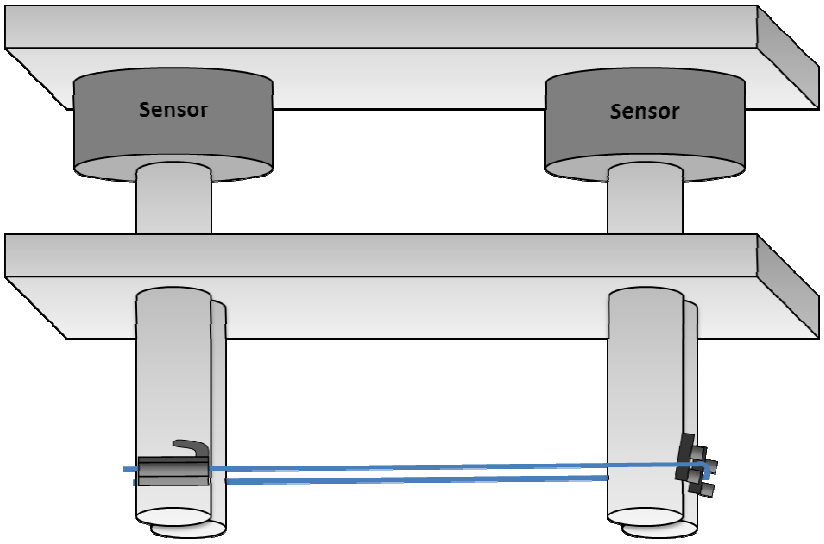

Figure 8

The wires to be tested were manufactured and prepared by Ultimate Wireforms, Inc. in Bristol, CT. The wire materials included NiTi (austenitic at room temperature) and CNA. The wire sizes of each material included 0.016" x 0.022", 0.017" x 0.025", and 0.021" x 0.025". One set of symmetrical V-bends (right and left sides) were placed in each wire, and each bend was placed to be 150º. There were eight possible positions

for the V-bends. The mesio-distal position V-bends were measured with an a/L ratio, where a is the distance between the central incisor bracket and the apex of the V-bend, and L is the interbracket distance between the first molar and central incisor brackets (both distances measured along the perimeter of the arch wire). An a/L ratio of 0.0 would represent a bend immediately adjacent to the incisor bracket, and each successive bend (a/L = 0.1, 0.2, etc.) would be spaced 3.8 mm away from the previous bend ending with a/L = 1.0, which would represent a bend immediately adjacent to the molar bracket. Due to limitations of the manufacturing process, bends closer to the incisor bracket than a/L = 0.3 were not produced nor tested. In Figure 9, each pair of right and left arrows shows a bend position that was present on one wire.

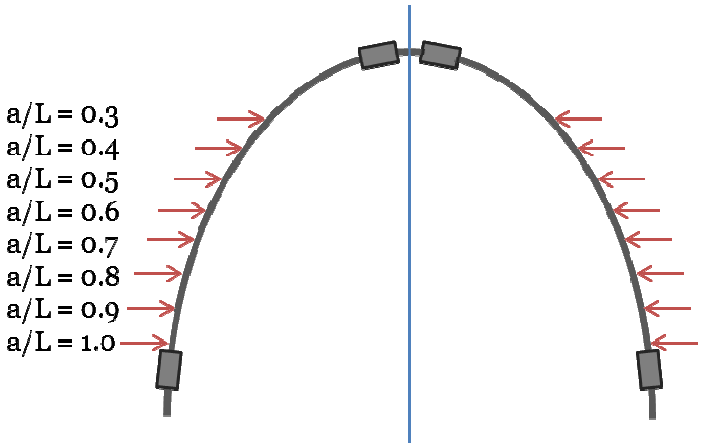

Figure 9

Experimental Procedure

1. Before any wire was engaged in the brackets, the software program was started to set the "zero point" of both sensors. At this time, the software program displayed each of the three force and three moment values at each sensor in real-time, and

all six measurements at each sensor were confirmed to be negligible values (forces < 1 g and moments < 10 g·mm) before continuing.

2. One wire sample was engaged into the first molar and central incisor brackets, representing a 2x2 appliance. The wire was held in place using the passive self-ligation system on the central incisor brackets. Figure 10 shows an example of a wire inserted into the testing apparatus before it is engaged in the incisor brackets.

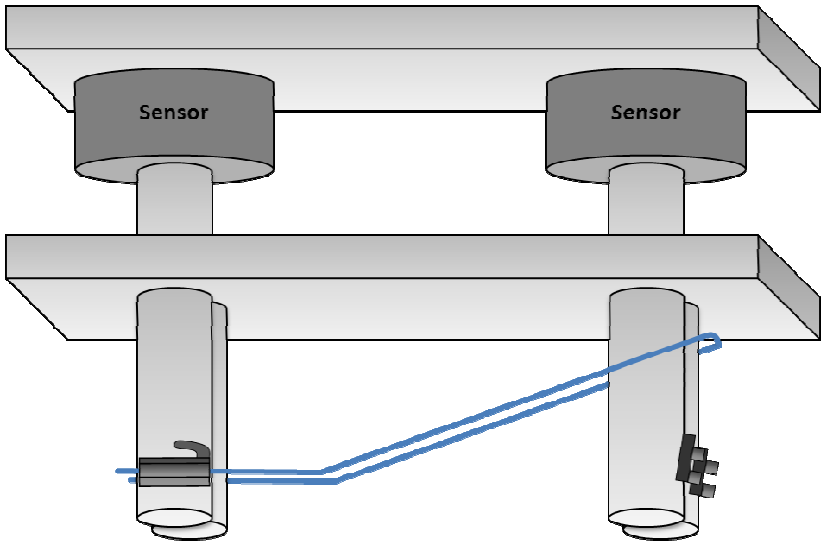

Figure 10

3. The recording feature of the software program was run for a five second measurement cycle, in which the three force and three moment components from each of the two sensors was recorded. Each cycle generated 50 readings over the five second period for each component (F_x, F_y, F_z, M_x, M_y, M_z). Thus, for each individual wire sample, there were twelve associated measurements (six components at two sensors) with 50 readings per measurement, and these were recorded to a Microsoft Excel spreadsheet.
4. The wire sample was removed from the apparatus, and the computer program was stopped.

5. Steps 1-4 were repeated for each wire sample.

For each combination of wire specifications (wire material, wire dimension, and position of v-bend), ten samples were measured, which resulted in 480 total samples.

Mathematical Analysis

The total force and total moment experienced by each sensor at the center of the sensor plate was represented by their three orthogonal components: F_x, F_y, and F_z represented the forces along the x-axis, y-axis, and z-axis, respectively; and M_x, M_y, and M_z represented the moments around the x-axis, y-axis, and z-axis, respectively. The 3D coordinate system relative to the maxillary dental arch consisted of the x-axis running lateral-medial, the y-axis running anterior-posterior, and the z-axis running occlusal-gingival. Since it is only clinically relevant to determine the force system applied at the brackets rather than the sensors, the initial measurements were converted mathematically to the force and moment values experienced by the bracket using the equations shown in Table 3. The distance values (d_x, d_y, and d_z) represented the 3D position of the center of the bracket pad in relation to the center of the sensor plate. These values are shown for each sensor in Table 4. The positive/negative sign convention simply indicated the specific direction along each axis according to the 3D coordinate system used throughout the study.

Measured Values (at sensor):	Calculated Values (at bracket):
F_x M_x	$F_x(\text{bracket}) = F_x$ $M_x(\text{bracket}) = M_x - (F_y d_z - F_z d_y)$
F_y M_y	$F_y(\text{bracket}) = F_y$ $M_y(\text{bracket}) = M_y - (F_x d_z - F_z d_x)$
F_z M_z	$F_z(\text{bracket}) = F_z$ $M_z(\text{bracket}) = M_z - (F_x d_y - F_y d_x)$

Table 3

Sensor 1 – Incisor	Sensor 2 – Molar
d_x = 0.442 mm	d_x = 3.908 mm
d_y = -3.144 mm	d_y = -0.689 mm
d_z = -30.5 mm	d_z = -30.5 mm

Table 4

The force systems at the brackets were described in two different coordinate systems: global and individual tooth. The global coordinate system consisted of a set of x-, y-, and z-axes at each tooth, and these axes corresponded to directions relative to the entire maxillary arch (lateral-medial, anterior-posterior, occlusal-gingival). The individual tooth coordinate system consisted of a set of x-, y-, and z-axes, but the axes at each tooth corresponded to directions relative to the specific position of that tooth (mesial-distal, facial-palatal, occlusal-gingival). This analysis was included to allow examining the 3D force systems in terms of the directions relevant to the movement of each tooth individually. The incisor coordinate system was rotated 8º in the occlusal plane in

relation to the global coordinate system, and the molar coordinate system was rotated 80º in the occlusal plane in relation to the global coordinate system. This concept is demonstrated in Figure 11.

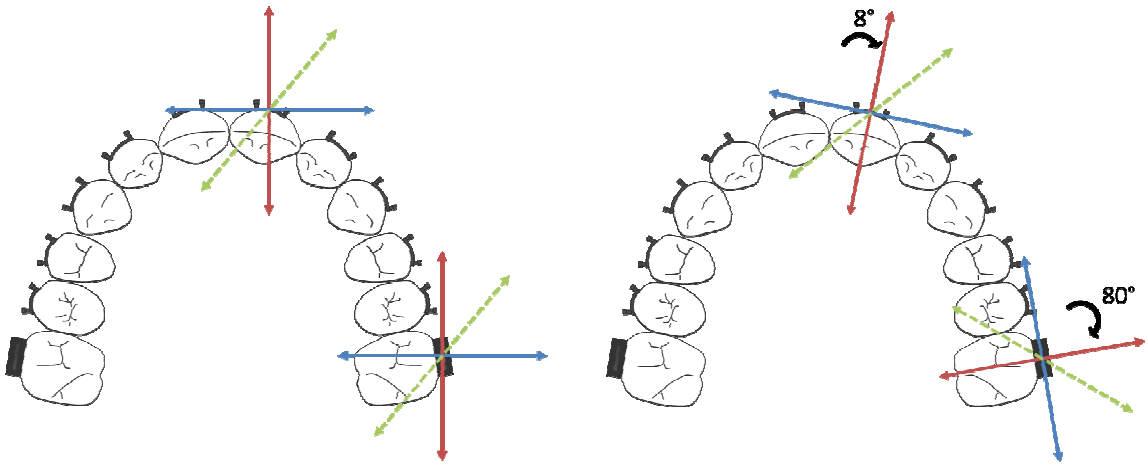

Global Coordinate System Individual Tooth Coordinate System

Figure 11

Table 5 displays the calculations used to determine the force and moment values according to the incisor coordinate system (ICS) and molar coordinate system (MCS). For simplicity in Table 5, the force and moment values F_x, F_y, F_z, M_x, M_y, and M_z represent F_x(bracket), F_y(bracket), F_z(bracket), M_x(bracket), M_y(bracket), and M_z(bracket) from Table 3, respectively.

Sensor 1 – Incisor (8° rotation)	**Sensor 2 – Molar (80° rotation)**
$F_x(ICS) = F_x \cos(-8°) + F_y \cos(82°)$	$F_x(MCS) = F_x \cos(-80°) + F_y \cos(10°)$
$F_y(ICS) = F_x \sin(-8°) + F_y \sin(82°)$	$F_y(MCS) = F_x \sin(-80°) + F_y \sin(10°)$
$F_z(ICS) = F_z$	$F_z(MCS) = F_z$
$M_x(ICS) = F_x \cos(-8°) + F_y \cos(82°)$	$M_x(MCS) = F_x \cos(-80°) + F_y \cos(10°)$
$M_y(ICS) = F_x \sin(-8°) + F_y \sin(82°)$	$M_y(MCS) = F_x \sin(-80°) + F_y \sin(10°)$
$M_z(ICS) = M_z$	$M_z(MCS) = M_z$

Table 5

Table 6 shows the sign convention used while calculating the forces and moments for both the global and individual tooth coordinate systems. Note that for the global coordinate system, the directions used to describe the forces and moments acting on the individual teeth are given relative to the entire maxillary arch. In contrast, for the individual tooth coordinate system, the directions are given relative to the specific tooth in question.

	Global	**Individual Tooth**

	Coordinate System	Coordinate System
+ F_x	Lateral	Distal
- F_x	Medial	Mesial
+ F_y	Posterior	Palatal
- F_y	Anterior	Facial
+ F_z	Gingival	Gingival
- F_z	Occlusal	Occlusal
+ M_x	Tip Anterior	Tip Facial
- M_x	Tip Posterior	Tip Palatal
+ M_y	Tip Lateral	Tip Distal
- M_y	Tip Medial	Tip Mesial
+ M_z	Mesial In	Mesial In
- M_z	Mesial Out	Mesial Out

Table 6

Statistical Methods

Statistical analyses were performed using Graph Pad Prism (GraphPad Software, Inc., La Jolla, CA). Analyses of variance (ANOVA) were used to examine differences in the curves for each force or moment component across the six arch wires used: NiTi 0.016" x 0.022", NiTi 0.017" x 0.025", NiTi 0.021" x 0.025", CNA 0.016" x 0.022", CNA 0.017" x 0.025", and CNA 0.021" x 0.025". Each curve was considered a data set and consisted of the mean values of the force or moment component at each a/L ratio (0.3 – 1.0). Subsequent post-hoc analyses using Bonferroni's Multiple Comparison Test were used to compare each wire against each other wire, but only those comparisons which examined the specific variables were recorded. Thus, for each wire size, the NiTi and CNA wire were tested against each other, and for each wire material, the three wire sizes were tested against one another. By convention, any significant differences were reported by indicating p-values < 0.05.

Results:

For each individual wire sample, 50 readings over a five second period were recorded for each component (F_x, F_y, F_z, M_x, M_y, and M_z) at each sensor (incisor and molar). The equations mentioned in Tables 3-5 were applied to each reading to determine the force system at the position of the brackets. Next, for each set of 50 values, the mean was calculated to generate a set of twelve values (six components at two sensors) for each of the two coordinate systems. Any variations among the 50 values in a particular set were negligible as they represented very minute fluctuations in the electronics of the sensor or software program; the standard deviations for the mean values were < 0.75 g for the forces and < 5 g·mm for the moments.

Each set of twelve values described the complete 3D initial force system applied at both brackets. Although only the pegs representing the right central incisor and first molar were connected to sensors, it was assumed that the forces and moments acting at the pegs representing the left central incisor and first molar were symmetrical about the sagittal plane of the dental arch. Ten samples were tested for each combination of wire specifications (wire material, wire dimension, and position of v-bend) to consider variations caused by factors such as operator error, slight differences in wire insertion or activation, and differences in the exact position or angle of the v-bends for each wire sample. Thus, for each group of ten wire samples with the same specifications, the mean and standard deviations were calculated for each force and moment component in both coordinate systems. Each point on the graphs shown below represents the mean value of the ten wire samples in that group, and the error bars represent one standard deviation above and below this mean.

When comparing the graphs displaying the force systems relative to the global coordinate system with those relative to the individual tooth coordinate system, it was clear that they were very similar in the magnitudes, directions, and patterns of the forces and moments for each wire type. The small differences are due to the fact that the x- and y-axes for both coordinate systems were rotated by only a small amount in relation to one another. For example, at the incisor bracket, an anterior force in the global coordinate system differed from a facial force in the incisor coordinate system by only 8°. Similarly, at the molar bracket, a lateral force in the global coordinate system differed from a buccal force in the molar coordinate system by only 10° (90° - 80°). These minor differences are true for all of the forces and moments associated with the x- and y-axes. The z-axes in both systems were identical, and therefore, the graphs representing forces along the z-axis and moments around the z-axis are exactly identical for both coordinate systems. Due to the similarity in results for both coordinate systems, only the force systems in relation to the individual tooth coordinate system will be discussed in detail in this report. However, the data for the global coordinate system are shown in the appendix section, and the discussion can be similarly applied to those results.

Although it is very important to pay close attention to the sign convention of each of the force and moment component when applying mathematical calculations, it is not relevant to consider the force system in those terms clinically. Rather, it is simpler to imagine the forces and moments by the type of tooth movement that would likely occur. For example, + F_z and - F_z forces are better understood as extrusive and intrusive forces, respectively. Thus, each of the graphs is labeled to describe the direction of tooth movement likely to occur above or below the horizontal axis, and the positive and

negative signs can be ignored. A point close to the horizontal axis (either above or below) signifies a force or moment with a low magnitude, and a point farther from the horizontal axis (either above or below) signifies a force or moment with a higher magnitude. Furthermore, for each of the graphs, a line representing the incisor bracket is paired with a line representing the molar bracket. These pairings were based on which combination of force or moment components at both of the brackets were most closely related when considering that the force system is in equilibrium. For example, a force in the facial/palatal direction on the incisor would be most closely associated with a force in the mesial/distal direction on the molar because these forces would be almost parallel to one another. This is due to the relative positions and orientations of the teeth around the dental arch. Conversely, a force in the mesial/distal direction on the incisor and a force in the mesial/distal direction on the molar would be almost perpendicular to one another, and therefore less associated in terms of an equilibrium force system.

Figures 12 – 23 show a series of graphs displaying the magnitude and direction of a particular force or moment component versus the a/L ratio in relation to the individual tooth coordinate system. The graphs are grouped by the wire type: NiTi 0.016" x 0.022", NiTi 0.017" x 0.025", NiTi 0.021" x 0.025", CNA 0.016" x 0.022", CNA 0.017" x 0.025", and CNA 0.021" x 0.025". The vertical axes are labeled with the direction of tooth movement above and below the horizontal axis. In cases where the descriptions differ for the incisor bracket and molar bracket, they are labeled with (I) or (M), respectively. The horizontal axes are labeled with the a/L ratio. As previously described, an a/L ratio of 0.3 represents a bend at 30% of the interbracket distance from the incisor bracket, and this is the bend closest to the incisor bracket that was tested. As the a/L ratio

increases, the bend is positioned progressively farther from the incisor bracket. At a/L = 1.0, the bend is at 100% of the interbracket distance from the incisor bracket, and thus, it is adjacent to the molar bracket.

Figure 12: Force components, NiTi 0.016" x 0.022"

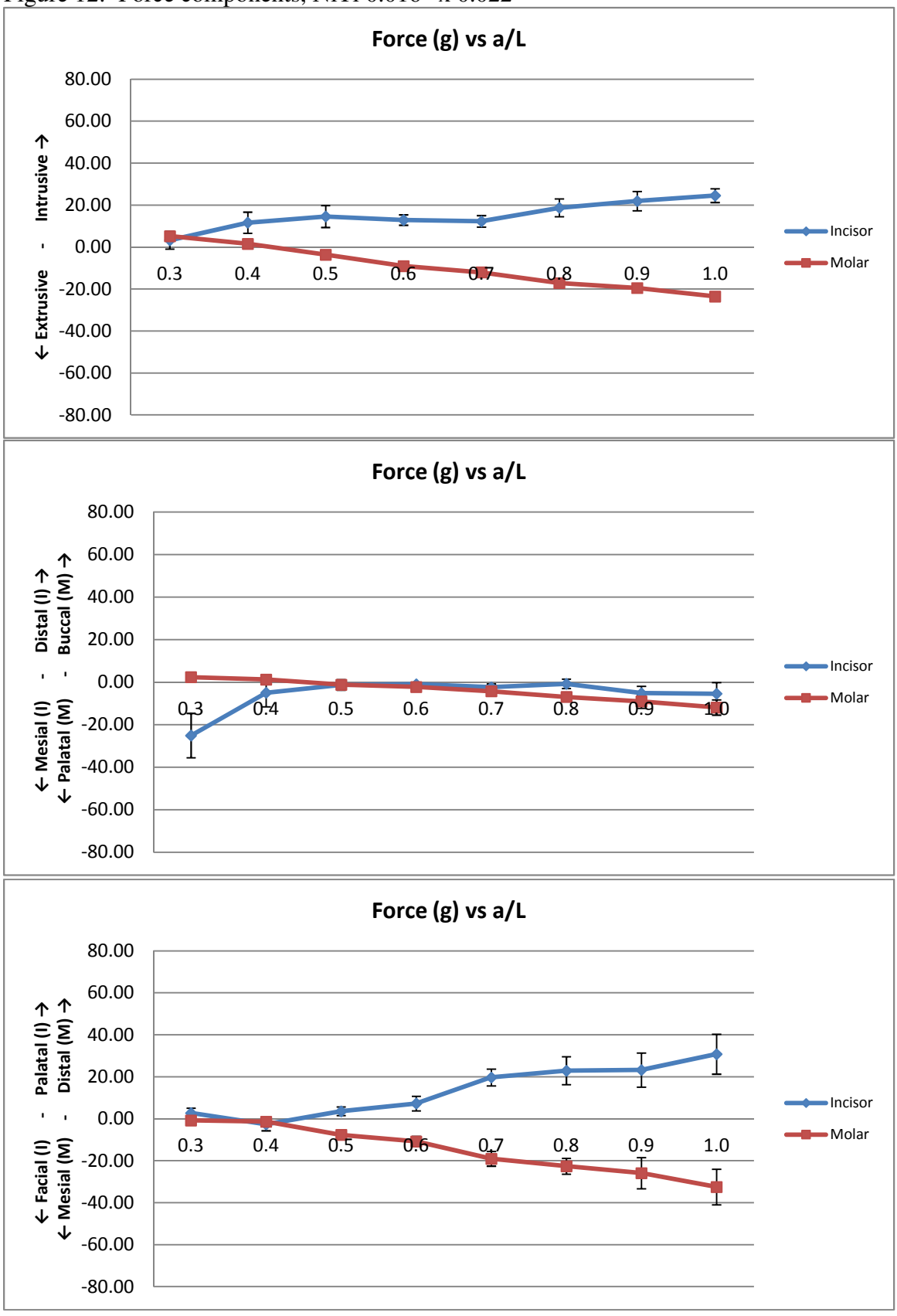

Figure 13: Moment components, NiTi 0.016" x 0.022"

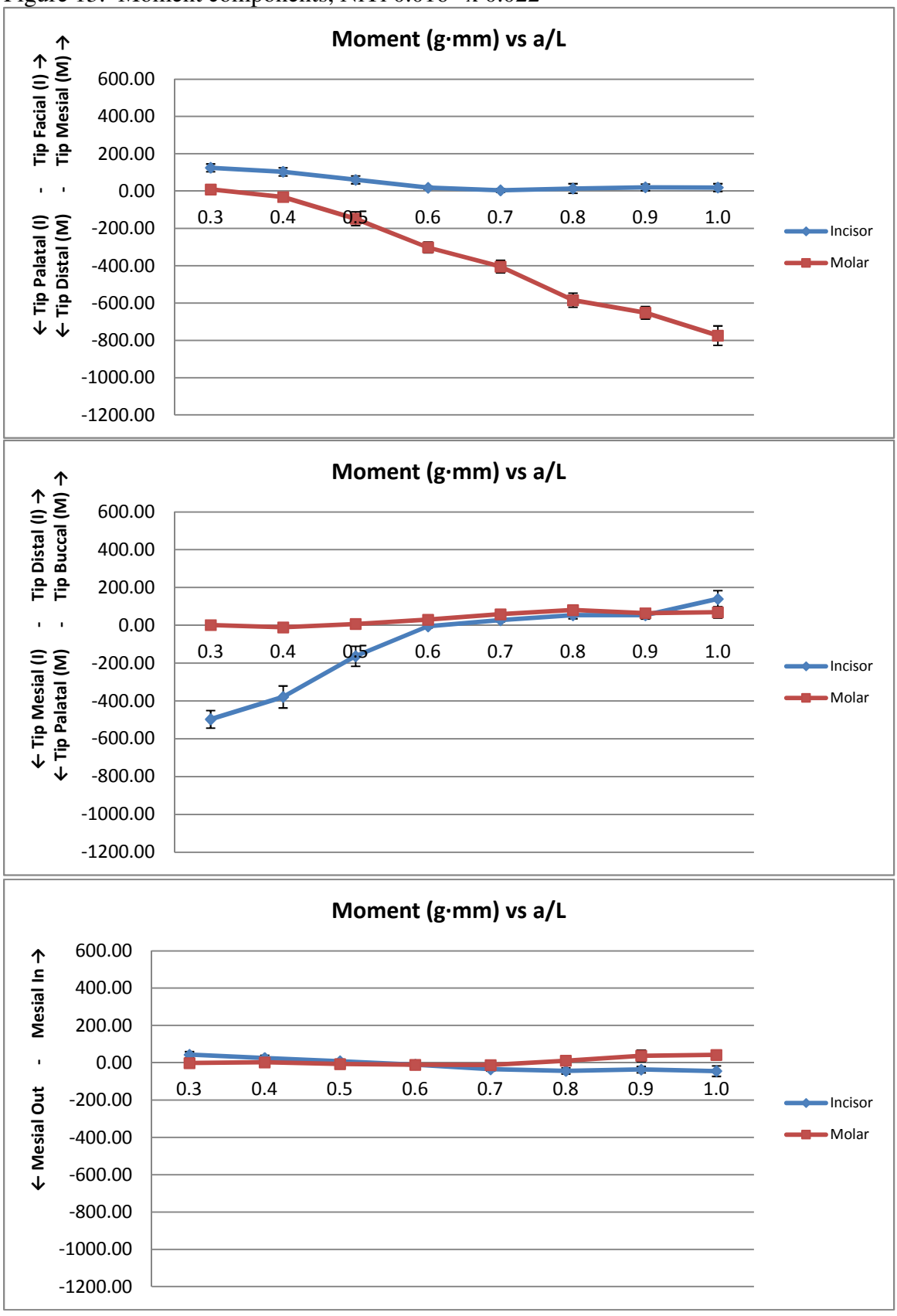

Figure 14: Force components, NiTi 0.017" x 0.025"

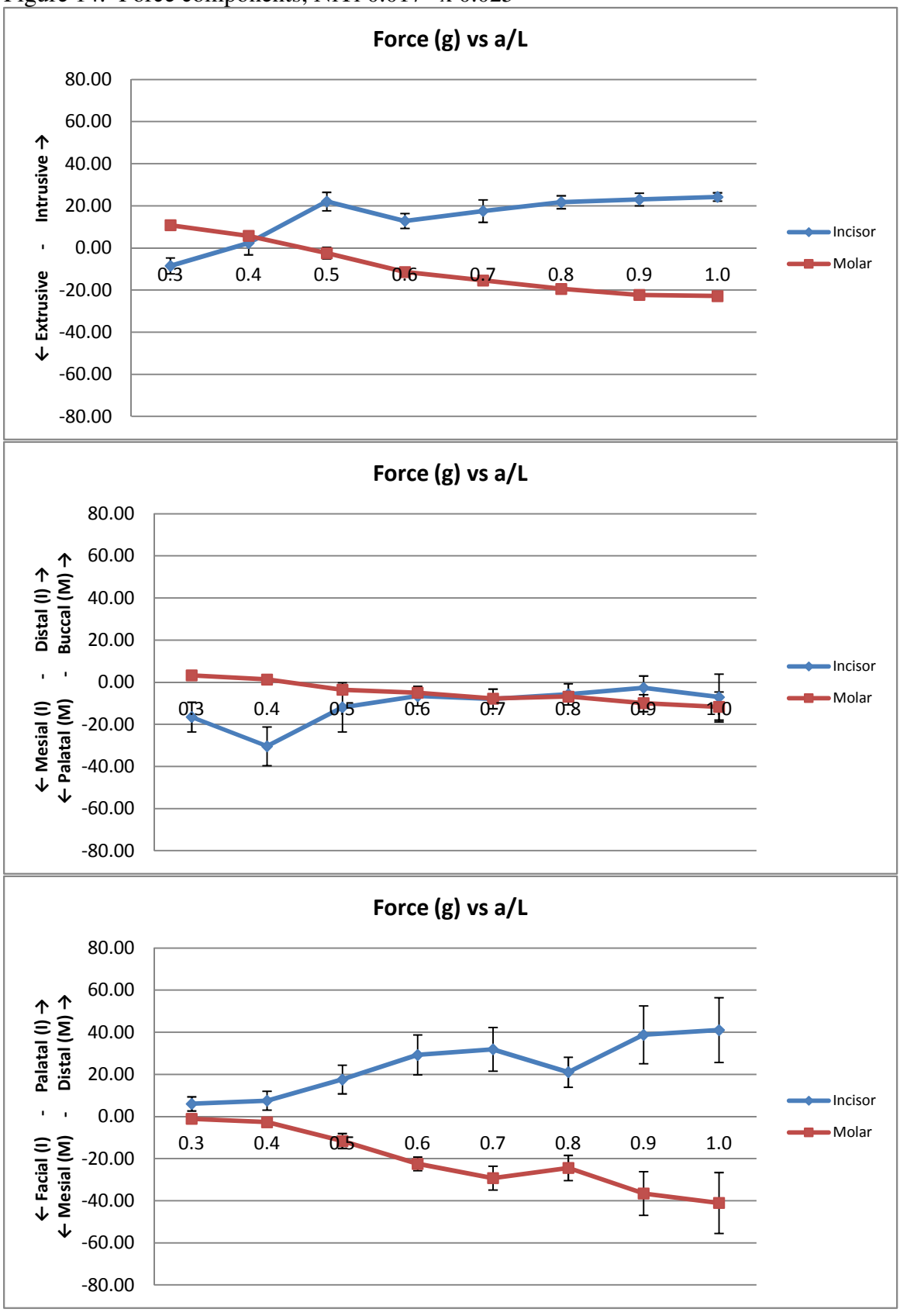

Figure 15: Moment components, NiTi 0.017" x 0.025"

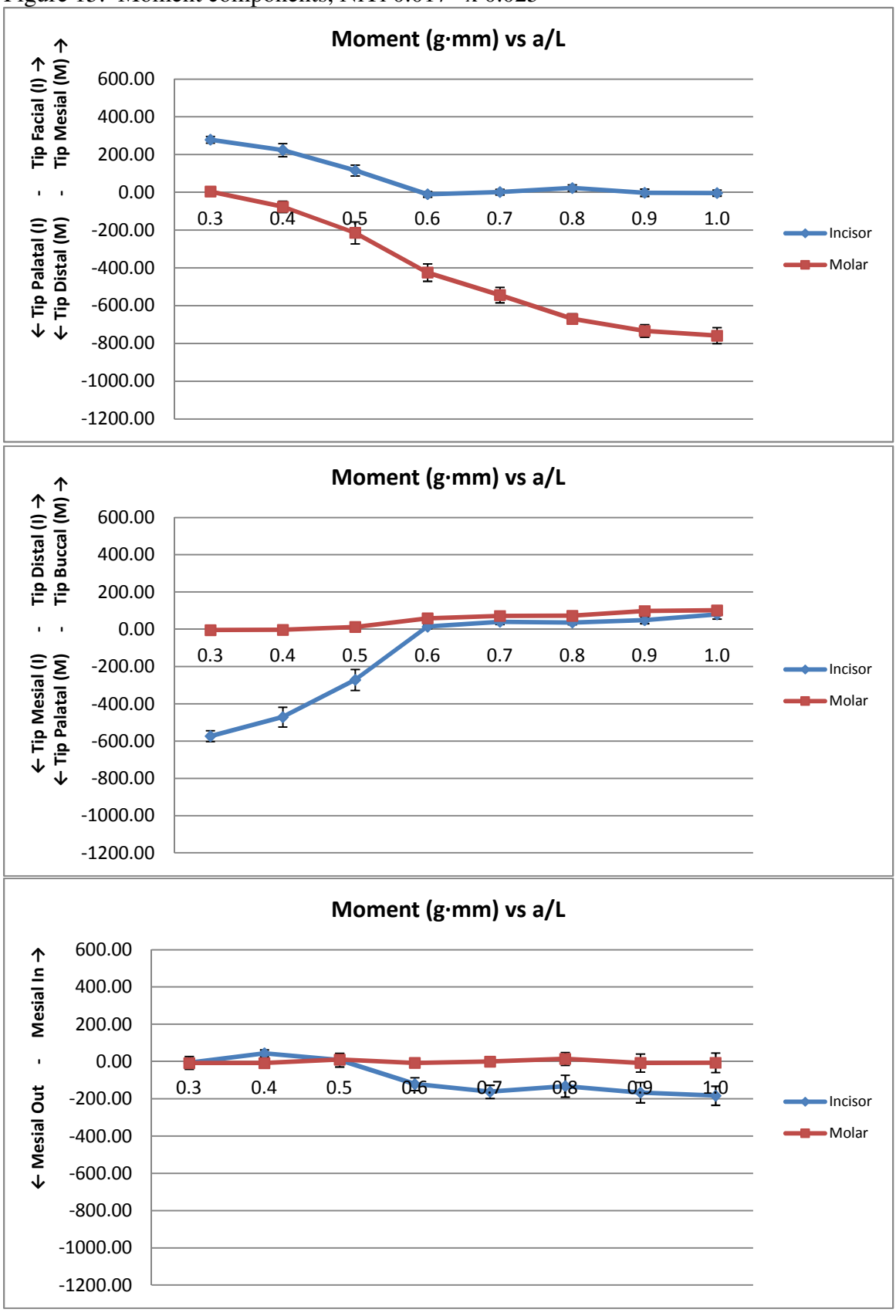

Figure 16: Force components, NiTi 0.021" x 0.025"

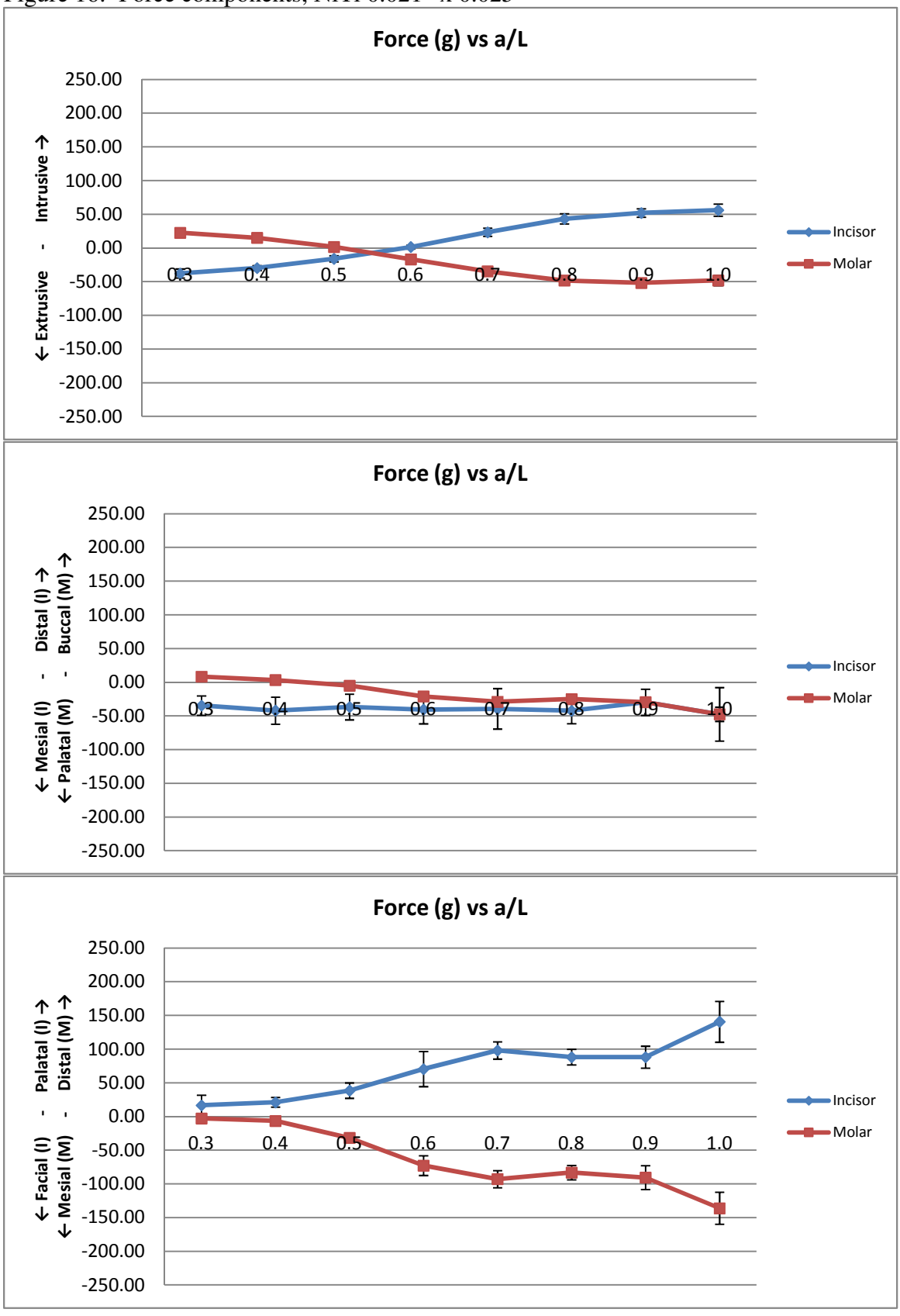

Figure 17: Moment components, NiTi 0.021" x 0.025"

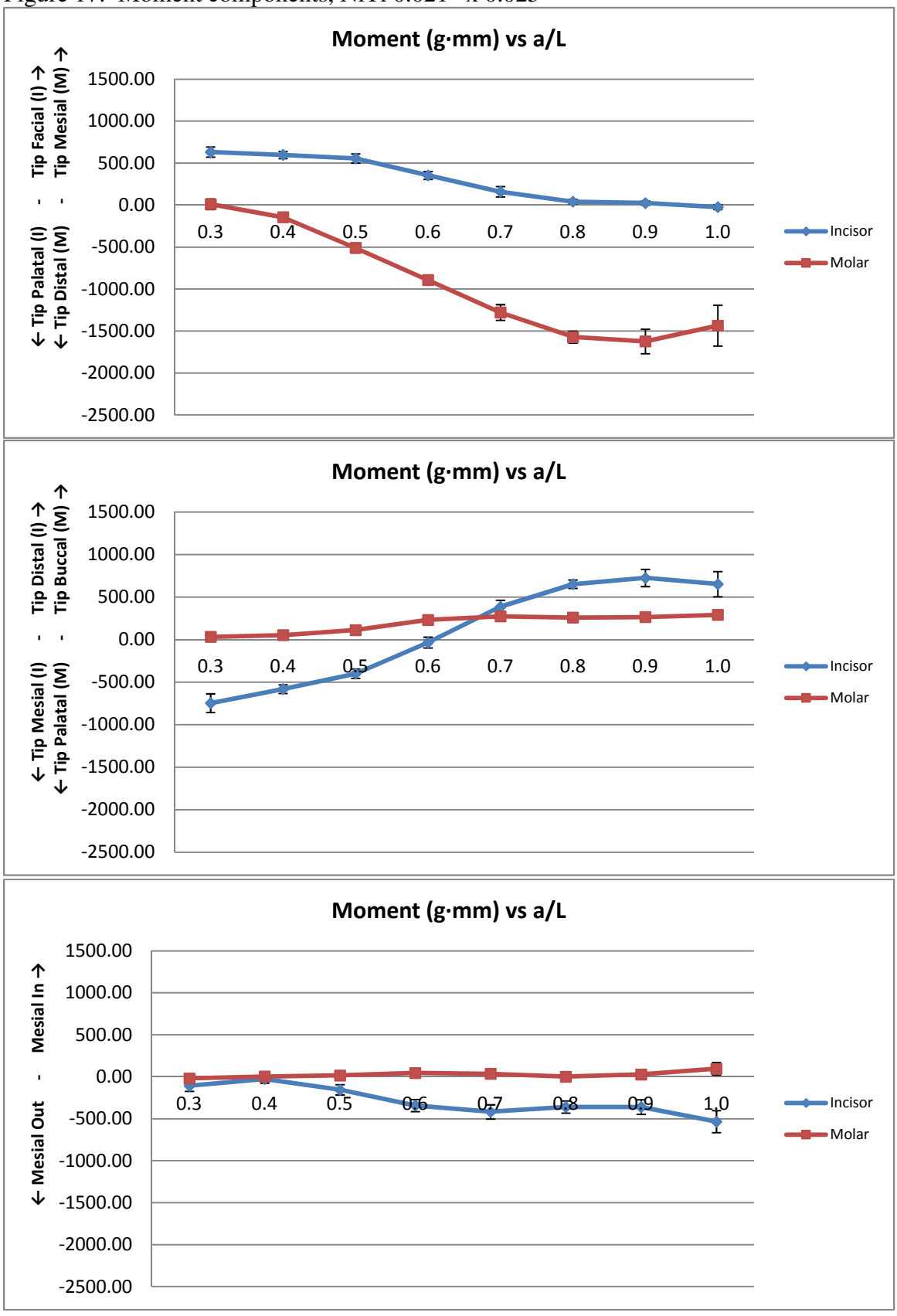

Figure 18: Force components, CNA 0.016" x 0.022"

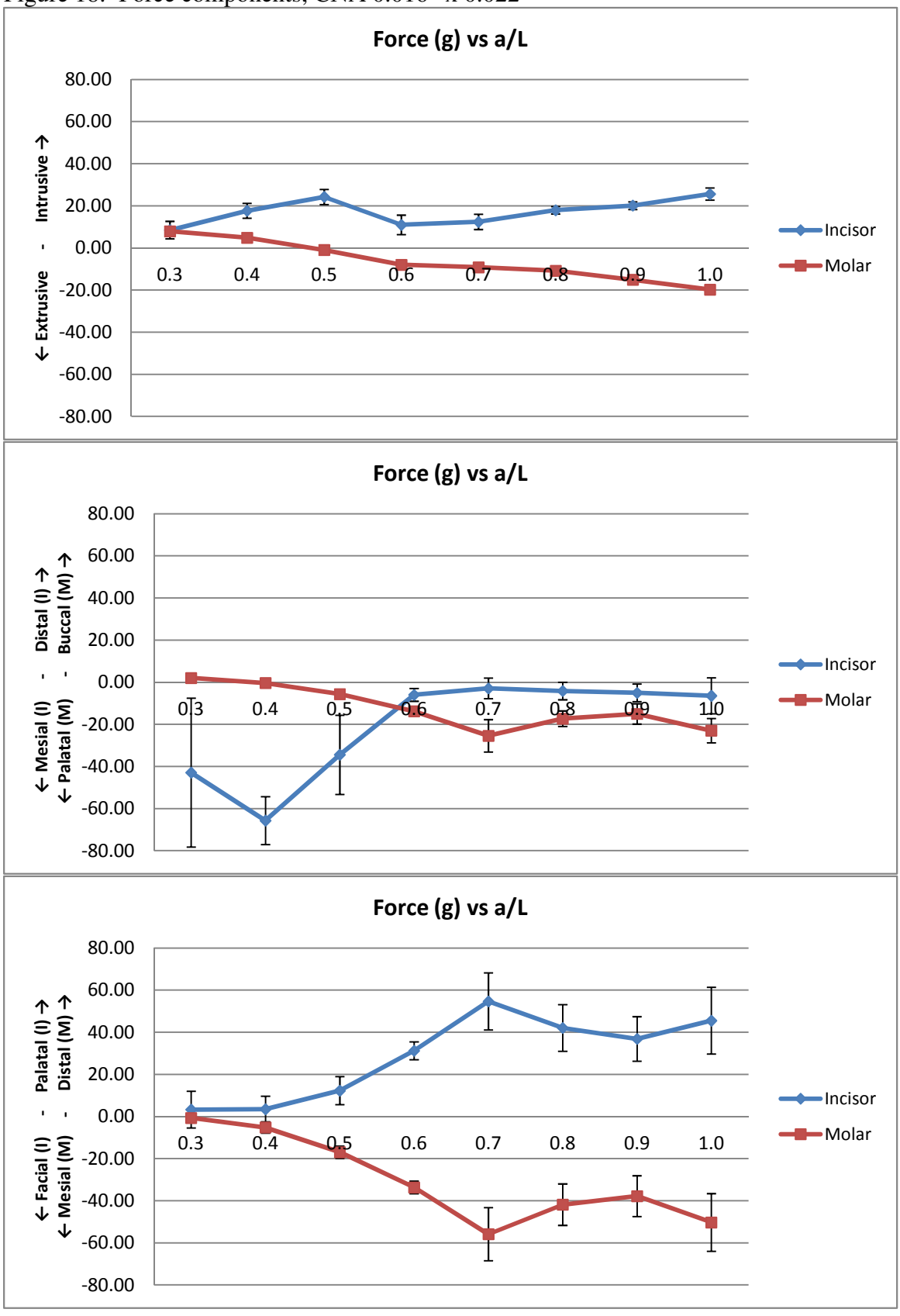

Figure 19: Moment components, CNA 0.016" x 0.022"

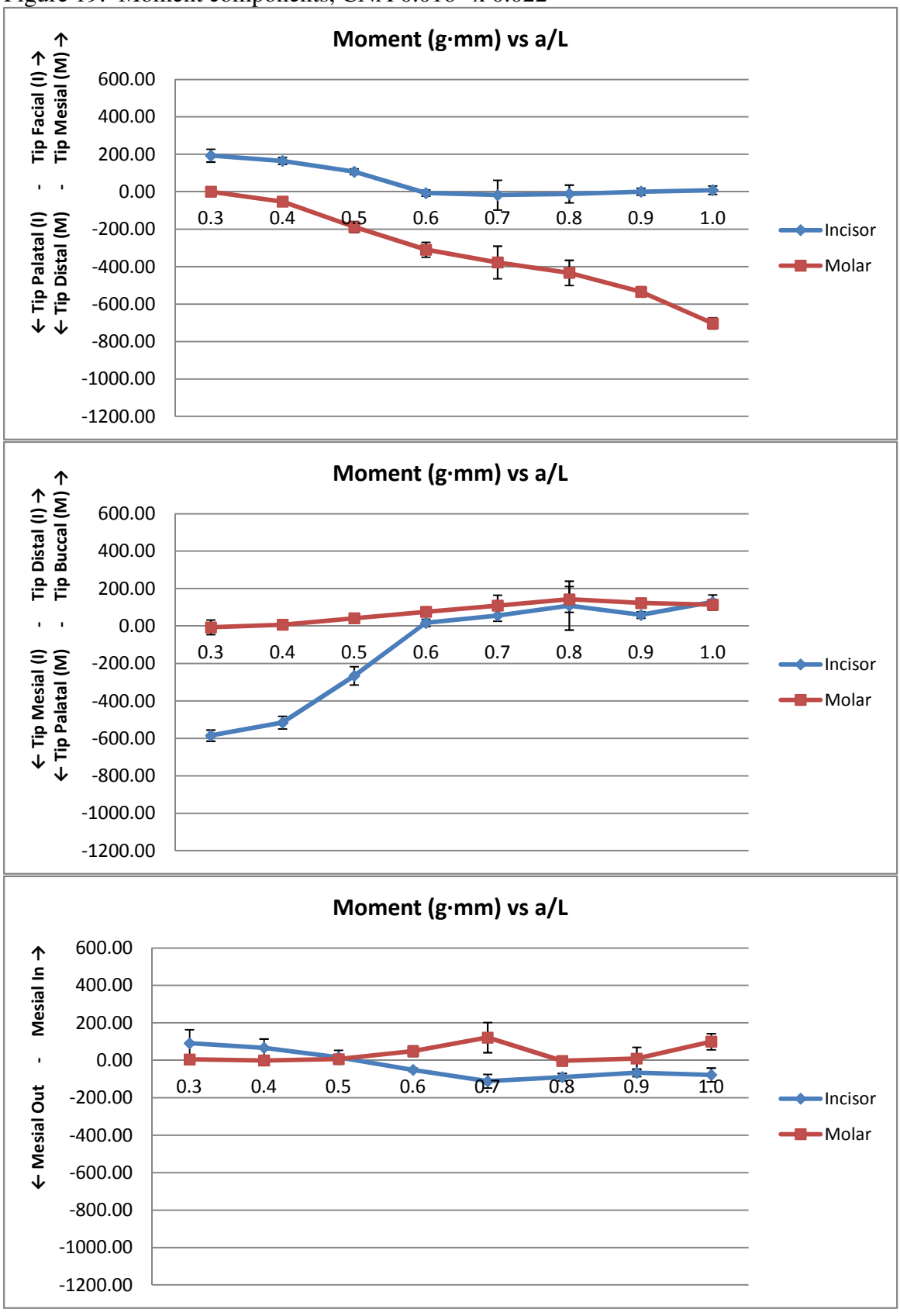

Figure 20: Force components, CNA 0.017" x 0.025"

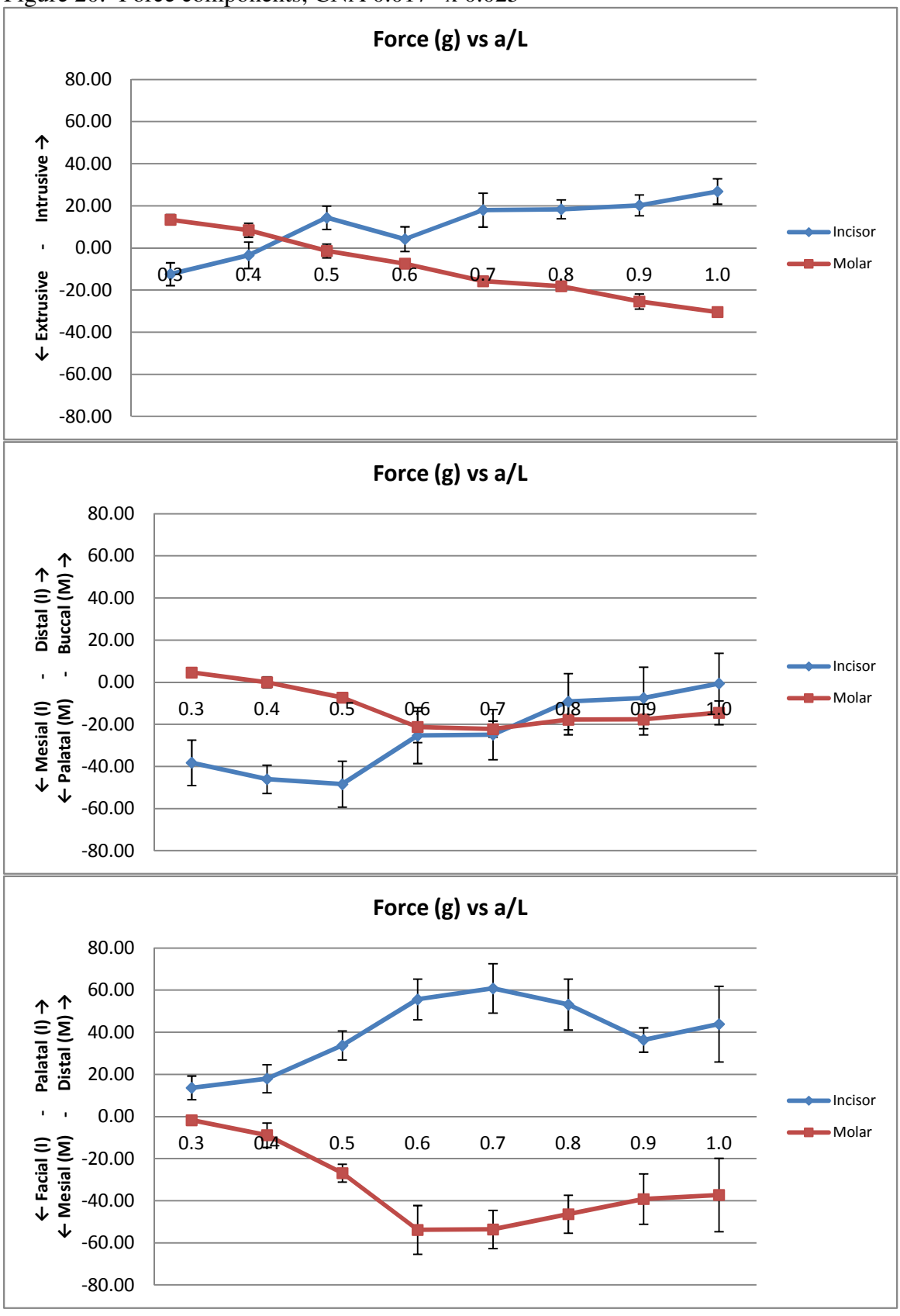

Figure 21: Moment components, CNA 0.017" x 0.025"

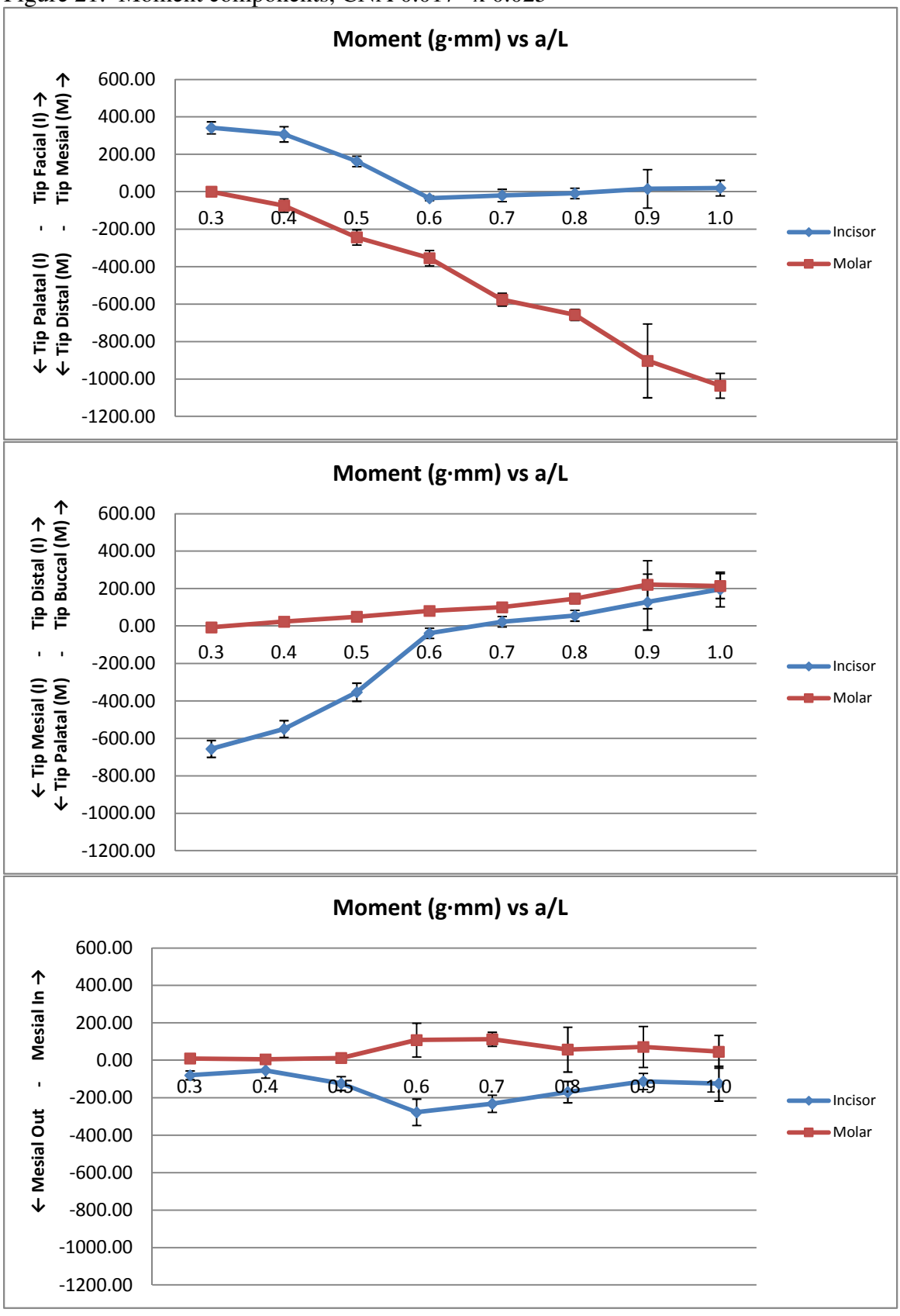

Figure 22: Force components, CNA 0.021" x 0.025"

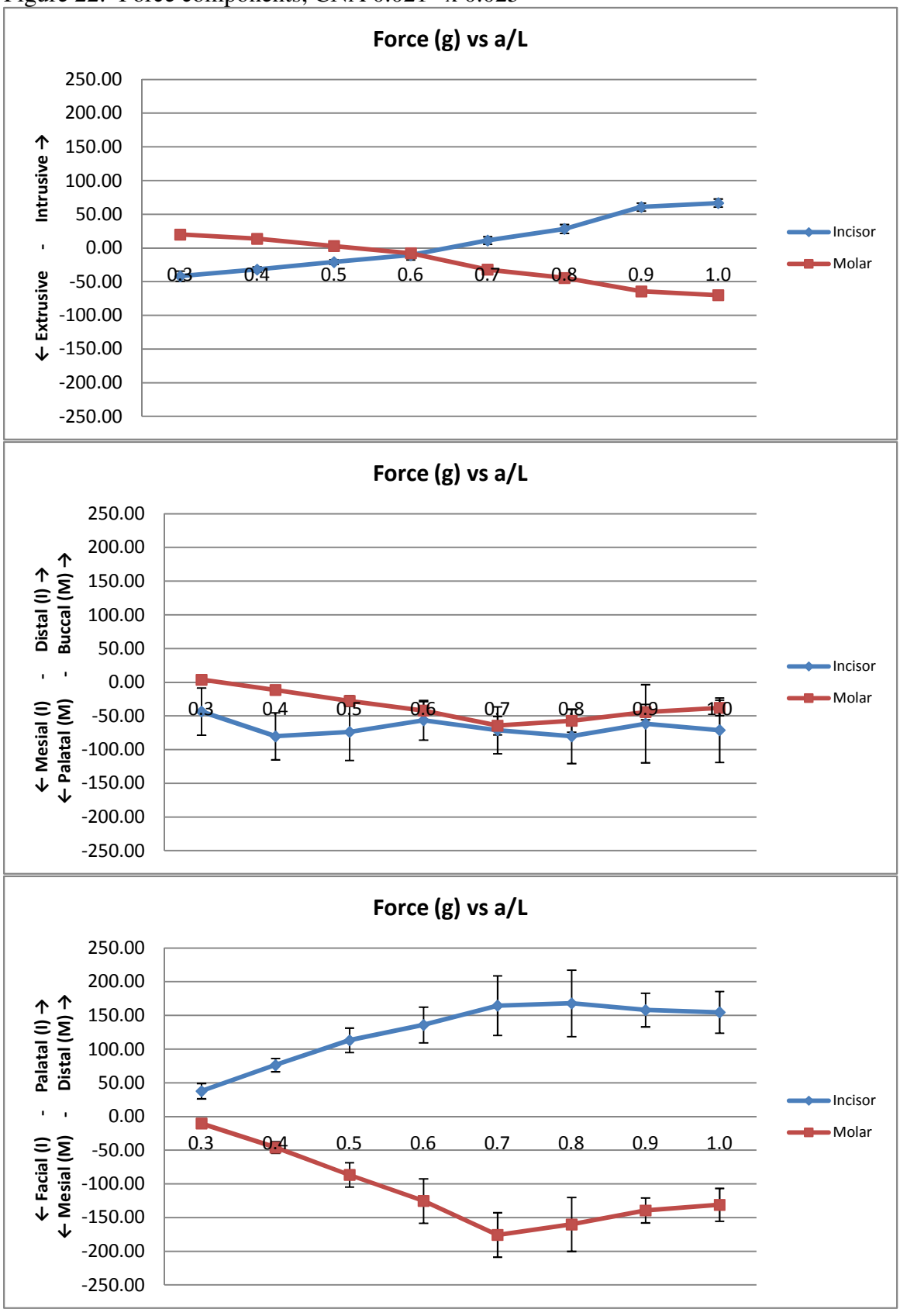

Figure 23: Moment components, CNA 0.021" x 0.025"

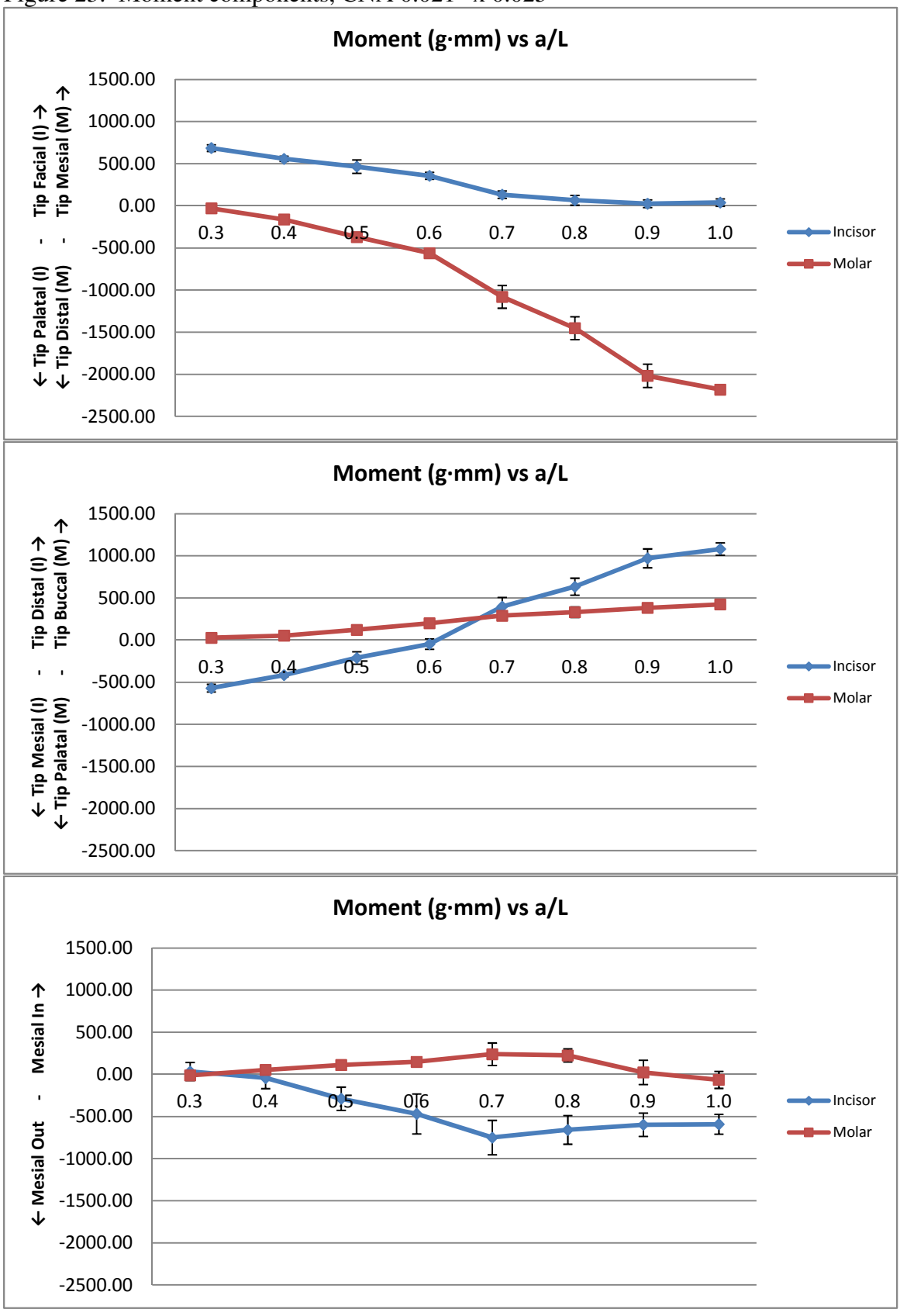

For the incisor bracket and molar bracket, Tables 7 and 8, respectively, show the results of the post-hoc analyses using Bonferroni's Multiple Comparison Test for the force and moment components. Each comparison is labeled as Yes if there was statistical significance ($p < 0.05$).

	Forces			Moments		
	Mesial / Distal	**Facial / Palatal**	**Extrusive / Intrusive**	**Tip Palatal / Tip Facial**	**Tip Mesial / Tip Distal**	**Mesial Out / Mesial In**
Comparisons of Wire Material						
CNA 16x22 vs NiTi 16x22	No	No	No	No	No	No
CNA 17x25 vs NiTi 17x25	No	No	No	No	No	No
CNA 21x25 vs NiTi 21x25	Yes	Yes	No	No	No	No
Comparison of Wire Dimensions in CNA wires						
CNA 16x22 vs CNA 17x25	No	No	No	No	No	No
CNA 16x22 vs CNA 21x25	Yes	Yes	No	No	No	Yes
CNA 17x25 vs CNA 21x25	Yes	Yes	No	No	No	Yes
Comparisons of Wire Dimensions in NiTi wires						
NiTi 16x22 vs NiTi 17x25	No	No	No	No	No	No
NiTi 16x22 vs NiTi 21x25	Yes	Yes	No	No	No	Yes
NiTi 17x25 vs NiTi 21x25	Yes	Yes	No	No	No	No

Table 7 (Incisor bracket)

	Forces			Moments		
	Palatal / Buccal	**Mesial / Distal**	**Extrusive / Intrusive**	**Tip Distal / Tip Mesial**	**Tip Palatal / Tip Buccal**	**Mesial Out / Mesial In**
Comparisons of Wire Material						
CNA 16x22 vs NiTi 16x22	No	No	No	No	No	No
CNA 17x25 vs NiTi 17x25	No	No	No	No	No	No
CNA 21x25 vs NiTi 21x25	No	No	No	No	No	No
Comparison of Wire Dimensions in CNA wires						
CNA 16x22 vs CNA 17x25	No	No	No	No	No	No
CNA 16x22 vs CNA 21x25	Yes	Yes	No	No	Yes	No
CNA 17x25 vs CNA 21x25	Yes	Yes	No	No	No	No
Comparisons of Wire Dimensions in NiTi wires						
NiTi 16x22 vs NiTi 17x25	No	No	No	No	No	No
NiTi 16x22 vs NiTi 21x25	No	No	No	No	Yes	No
NiTi 17x25 vs NiTi 21x25	No	No	No	No	No	No

Table 8 (Molar bracket)

Discussion:

The focus of this research was to experimentally determine the 3D force systems produced by vertical v-bends placed at different locations along the interbracket distance in a rectangular arch wire engaged in a 2x2 appliance. When v-bends are used clinically, the orthodontist is generally attempting to take advantage of the vertical forces and/or the moments in the same plane as these vertical forces. In fact, previous articles in the orthodontic literature regarding v-bends have described only these forces and moments. Thus, these studies were limited to a partial 2D force system in which the horizontal forces were ignored. However, based on the data from the current study presented above, it is evident that forces and moments in the other two planes tend to exist as well, and these components need to be considered as they may result in unwanted side effects. Although a vertical v-bend is placed in the sagittal plane, a complete 3D force system can be expected because of the curvature of an arch wire, which was not accounted for in the initial studies regarding v-bends. Due to this curve, the incisor and molar brackets are not positioned in the same plane, nor are they oriented parallel to one another. This arrangement can add complexity to the analyses of the force systems, but these in vitro experiments utilizing full arch wires can be more relevant clinically than those involving just two identical brackets arranged in a straight line and parallel.

By simply observing the graphs describing the initial force systems produced, it is clear that general trends exist as the v-bends are placed in different positions progressively along an arch wire. When examining the vertical (extrusive and intrusive) forces, each of the six wire types used produced a similar pattern. The closer the v-bend was to the molar bracket, the greater was the magnitude of an extrusive force on the

molar and of an intrusive force on the incisor. As the bend is moved away from the molar bracket, the magnitudes of both forces decrease until a certain point is reached where both forces are approximately zero. As the bend is moved farther from the molar beyond this point, the force magnitudes begin to progressively increase, but the directions of the forces are reversed to be extrusive on the incisor and intrusive on the molar. This point is analogous to a Class VI geometry, and it was located at different positions of the v-bend for each of the wires. For the 0.016" x 0.022" wires, this point was near a/L = 0.3; for the 0.017" x 0.025" wires, it was near a/L = 0.4 – 0.45; and for the 0.021" x 0.025" wires, it was near a/L = 0.55 – 0.6. According to the 2D data using two identical brackets in a straight line presented by Ronay et al., this point occurs when the v-bend is placed exactly halfway between the brackets. (8) When using an arch wire engaged in the first molars and the incisors, Burstone et al. predicted this point to occur when the bend is at a/L = 0.5, but this was under the assumptions that the forces existed in one plane only, there was full bracket engagement by the wire, and the wire was free to slide. (2) In their 3D finite element study, Isaacson et al. found this point to be slightly off center towards the molar (equivalent to a/L = 0.55 in the current study). (4) Thus, these results are similar to those found in the current in vitro study for the 0.021" x 0.025" wires. The observation that the bracket closer to the v-bend tended to have the extrusive force has been noted in the previous literature as well. (8)

Analyzing the moments present approximately in the sagittal plane (tip palatal/tip facial for the incisor and tip distal/tip mesial for the molar), every wire displayed a similar pattern. When the bend was nearest to the incisor bracket, the moment at the molar was about zero, and as the bend was moved toward the molar, this moment

increased in magnitude in the tip distal direction. At a/L = 0.3, the moment at the incisor was at its highest magnitude in that plane, and it was in the tip facial direction. As the a/L ratio increased, this moment decreased until it reached zero, and then it stayed at zero as the bend continued to be moved toward the molar bracket. For the 0.016" x 0.022" and 0.017" x 0.025" wires, the moment at the incisor was zero from a/L = 0.6 – 1.0, and for the 0.021" x 0.025" wires, this moment was zero from a/L = 0.8 – 1.0. When considering the 2D data, a position called the point of dissociation occurs, at which the moment becomes zero and only an intrusive force exists at the bracket farther from the bend, representing a Class IV geometry. (8) Using the mathematical analysis for the 2D bracket setup, this point was calculated to be at one-third of the interbracket distance, and Burstone et al. theorized that in an arch wire, the point of dissociation closer to the molar would be at one-third the distance from the molar. (2; 8) Using a finite element model of a dental arch, Isaacson et al. calculated the point of dissociation closer to the molar to be at 14% of the distance from molar. (4) In the current study, there was a striking difference as there was no single point of dissociation; rather, there was an entire range where the moment at the incisor bracket was zero. For the 0.021" x 0.025" wires, this range was the 20% of the wire closest to the molar, and for the other wires, it was the 40% of the wire closest to the molar. This pattern gives a significant implication for a clinician who wanted to place a 2 x 2 appliance with only an intrusive force at the incisors and no moment. Previously, it was thought that one would have to place the bend at a precise point to achieve this outcome, which can be difficult to measure and apply in a patient. According to the present study, though, the clinician has a whole range in which to the place the bend, so a small error in the position may still produce the

same result. However, it is important to remember that a small change in the position could produce different effects in other dimensions and at the other brackets. For example, although the incisor moment will stay at zero, a bend closer to the molar will produce a greater tip distal moment at the molar and greater vertical forces at both brackets. In the current study, the point of dissociation closer to the incisor, at which the moment at the molar is zero, was found to be at a/L = 0.3 for all of the wires. This is similar to the one-third point calculated from the 2D data by Burstone et al., and it is similar to finite element study by Isaacson who found this point to be at 37% of the distance from the incisor. (2; 4) In the present study, it was not possible to measure the effect of a v-bend closer to the incisor than a/L = 0.3. If it were possible, a similar flattening of the curve may have been seen for the moment at the molar for the range a/L = 0.0 – 0.3, but this cannot be confirmed without the experiments. Figure 24 compares the location of certain well-known geometries in the 2D data by Burstone et al. and in the current study using the CNA 0.017" x 0.025" wire as an example. For the 2D data, 1 and 2 represent two identical brackets, and for the current study, I and M represent the incisor and molar brackets, respectively.

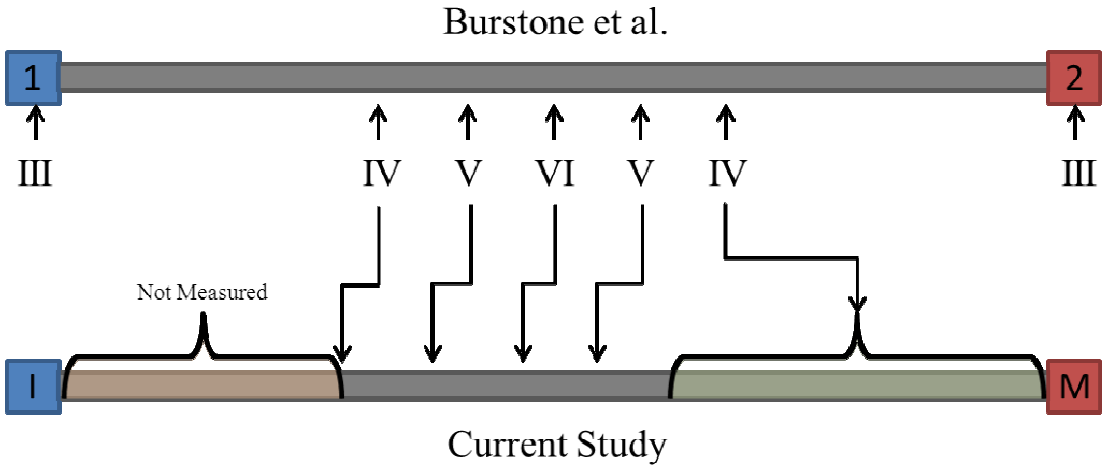

Figure 24

Note that in Figure 24, the pattern shown is similar for all of the 0.016” x 0.022” and 0.017” x 0.025” wires, especially the range in which the Class IV geometry exists. For the 0.021” x 0.025” wire, this range does not begin until the bend is moved to 80% of the interbracket distance from the incisor bracket. The reason for this is likely related to the play between the incisor bracket and the wires, which is caused by the discrepancy between the dimensions of the wire and the height of the bracket slot. In the sagittal plane, the moment at the incisors is due to a third order deflection, which can be referred to as torque. Since the wires do not fill the entire bracket slot, which is 0.022” x 0.028”, the torque is not expressed by the wire unless the deflection is greater than the amount of play. If the deflection is less than the amount of play, then the wire cannot apply a couple within the bracket because it cannot apply a force to both the upper and lower walls of the slot, and therefore, no moment can be generated. Consequently, a one couple force system is created, whose main components are equal and opposite vertical forces and a moment at the molar bracket only. When looking at the graphs, the highest moment at the incisor occurred when the bend was closest to the incisor bracket, and thus, the highest deflection of the wire was at this point as well. As the bend was moved away from the incisor, the deflection and the resulting moment decreased. The deflection decreased until it was less than the torque play, at which point the moment became zero. Using the formula presented by Joch et al. in their study on third order clearance, the play for 0.016” x 0.022” and 0.017” x 0.025” wires was 17.9° and 12.5°, respectively, while the play for 0.021” x 0.025” wires was only 2.3°. (22) Thus, while moving the bend away from the incisor, the point at which the deflection became less than the play occurred sooner for the smaller dimension wires because their play was greater. For the

0.021” x 0.025” wire, the deflection had to be much smaller (< 2.3°) for the Class IV geometry to occur, which is why the range did not begin until a/L = 0.8.

Regarding the orthodontic literature related to vertical v-bends, only the vertical forces and the associated moments (those in the sagittal plane) have been described. Thus, all of the other forces and moments observed in the present study cannot be compared to previous studies. When considering the horizontal forces approximately in the coronal plane of the dental arch (mesial/distal for the incisor and palatal/buccal for the molar), the force magnitudes and directions showed similar trends for the smaller dimension wires. The force magnitudes at the incisor were high in the mesial direction at the positions closest to the incisor (a/L = 0.3 – 0.5), and then they also leveled out to a relatively low value at a/L = 0.6 and farther. When the bend is close to the incisor bracket, the wire is essentially a two couple torqueing arch as described by Isaacson et al. (23) In this paper, the authors allude to this mesial force by stating that when a torqueing arch is left in the mouth for several months, the incisors will tend to experience a second order rotation in which the roots will diverge distally. (23) A mesial force at the incisor bracket would cause a rotation in this direction since the force would be acting below the CR of the tooth. This pattern was not seen for the 0.021” x 0.025” wires, in which the forces at the incisor bracket were in the mesial direction and remained relatively constant regardless of the position of the bend. At the molar bracket, the trends were similar for all of the wires. As the a/L ratio increased, the forces at the molar began at approximately zero and increased in the palatal direction. However, the magnitudes remained relatively low even at the extreme positions when considering they would cause arch constriction at the molars, so these forces may be of little clinical relevance.

Moving on to the moments approximately in the coronal plane of the dental arch (tip mesial/tip distal for the incisor and tip palatal/tip buccal for the molar), the patterns were similar to that of the forces in this plane. Again, the two smaller dimension wires produced a greater effect on the incisor brackets at the positions closest to the incisor (a/L = 0.3 – 0.5). For the molar bracket at all positions, and for the incisor bracket at a/L = 0.6 and farther, the moments were relatively low and likely not relevant clinically. Like the forces at the incisor bracket, the moments were highest at a/L = 0.3 in a tip mesial direction, and they decreased in magnitude as the bend was moved away. This moment would cause the same second order rotation in the incisor as mentioned above. When considering the configuration a torqueing arch would take when engaged in the incisor brackets, it is clear why the moments are in a tip mesial direction. Figure 25 demonstrates this concept by showing a torqueing arch before being engaged in the incisor brackets; due to the curve in the anterior part of the arch wire, the couple created by the deflection of the arch wire in the incisor brackets would produce tip mesial moments.

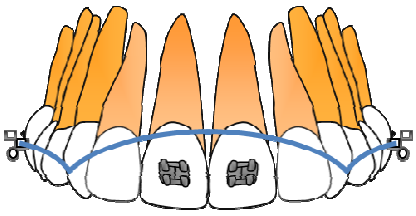

Figure 25

For the 0.021” x 0.025” wires, the moment at the incisor bracket was also in the tip palatal direction when the bend was closer to the incisor bracket, and it decreased to zero at a/L = 0.6. However, rather than remaining at zero beyond this point as it did in the other wires, the moment reversed and began to increase in the tip distal direction as the

bend moved to a/L = 1.0. The moment at the molar bracket was near zero at a/L = 0.3 and gradually increased until a/L = 1.0, but these moments were relatively low and would cause a tip buccal rotation of the molar.

When examining the horizontal forces approximately in the sagittal plane of the dental arch (facial/palatal for the incisor and mesial/distal for the molar), all of the wires displayed a similar pattern. At a/L = 0.3, the forces at both the incisor and molar brackets were around zero. As the a/L ratio increased to a/L = 0.7, the magnitude of the incisor force increased in the palatal direction, and the magnitude of the molar force increased in the mesial direction. As the a/L ratio continued to increase to a/L = 1.0, the force magnitudes fluctuated near the same value in the directions mentioned above. When one considers the forces at each bracket together, it is evident that the teeth are being pulled towards one another. This effect is likely caused by the activation and subsequent recoil of the v-bends after insertion of the wires. In other words, in order to insert a wire with a v-bend into the incisor and molar brackets, it must be "flattened" or activated. Since the wires have elastic properties, the v-bend would try to return to its original shape and "unflatten" after it is left engaged in the brackets. Thus, as the v-bend tries to "unflatten" or bring both legs of the v-bend closer together, the brackets in which the wire is engaged feel these forces, and they would try to bring the teeth closer together as well. To understand why these forces are higher when the bend is closer to the molar, one must note that these forces could be relieved if the wire was allowed to slide freely in the bracket slots with no friction. The wire being able to slide palatally in the incisor brackets would not decrease these forces because the wire would come into contact with the posterior wall of the bracket slot. However, if the wire was able to slide mesially in

the molar brackets, then these forces would be decreased. A major reason why the wire cannot slide mesially in the molar bracket is the friction between the wire and bracket. This friction is proportionally related to the normal forces between the wire and bracket, and these forces would include, among others, the vertical forces at the molar as well the forces that create the couple for the tip distal moment at the molar bracket. Because both the extrusive force and the tip distal moment at the molar bracket are increased as the a/L ratio increases, one can assume that the normal forces, and thus the friction, are also increased at these positions. Consequently, this higher friction would prevent the v-bend from "unflattening" and would cause the greater horizontal forces observed at both of the brackets at the higher a/L ratios.

Finally, when examining the moments in the occlusal plane (mesial out and mesial in for both teeth), there was again a slightly different pattern between the wire sizes. For the 0.016" x 0.022" and 0.017" x 0.025" wires, these moments at both brackets remained low and of little clinical significance at all positions. For the CNA 0.021" x 0.025" wire, there was a mesial in moment at the molar for a few of the positions, but these values were relatively low and likely insignificant clinically. The moment at the incisor increased from roughly zero at a/L = 0.3 to a/L = 0.7 in a mesial out direction. After a/L = 0.7, the magnitude decreased only slightly until a/L = 1.0. For the NiTi 0.021" x 0.025" wire, the moment at the molar remained close to zero for all positions, and the moment at the incisor increased steadily in the mesial out direction as the a/L ratio increased but still remained relatively low overall.

When examining the overall force systems produced by an arch wire, it is important to understand that all of the forces and moments in all three dimensions are

acting simultaneously on the brackets. Thus, when considering that the force system is at equilibrium, all of the forces and moments caused by the arch wire on both of the brackets must cancel out one another. In other words, when mathematically summing all of the forces and summing all of the moments, both must equal zero. Adding all of the moments present would be quite difficult because one would need to factor in the moments of the couples as well the moments of the forces. The graphs above only represent the moments of the couples, so the moments of the forces would need to be calculated in each dimension using the forces and the interbracket distances in each dimension. However, confirming that the forces sum to zero can be quick and simple using the graphs presented above. It is easy to see that all of the vertical forces roughly cancel out because the graphs describing these forces show somewhat symmetrical curves for the molar and incisor about the horizontal axis. An extrusive force on the molar would cancel an intrusive force on the incisor and vice versa. Similarly, the curves showing the facial/palatal forces on the incisor and mesial/distal forces on the molar are approximately symmetrical, so these forces also roughly cancel out one another. The curves are not exactly symmetrical because there could be small errors in the values due to operator error, fluctuations in the electronic signals of the sensors, etc., and due to the fact that the forces are not exactly parallel. For example, a mesial/distal force on the molar is not exactly parallel to a facial/palatal force on the incisor since they are 18° apart, but these can be used for a quick estimation. For the mesial/distal forces on the incisor and palatal/buccal forces on the molar, the curves are not symmetrical, but one must consider that these only represent the teeth on the right side of the dental arch. If the incisor and molar on the left side of the arch are assumed to experience symmetrical

forces about the sagittal plane, then all of these forces would be cancelled out by forces on the contralateral tooth. For example, a buccal force on the right molar would be cancelled out by a buccal force on the left molar of the same magnitude since they would be in opposite directions. Therefore, since the force systems must be at equilibrium, the graphs representing the forces can be quickly used to confirm that the measurements and calculations are somewhat accurate.

The results of the statistical tests used in the current study must be analyzed with caution mainly because for each of the force or moment components, the curves for each wire at each bracket were treated as a single data set. Consequently, the force and moment values were not compared individually for each specific a/L ratio, but rather, they were compared as one specific curve versus another curve of the same force or moment component. Nonetheless, certain conclusions can be drawn regarding the two variables: wire material (CNA and NiTi) and wire dimensions (0.016" x 0.022", 0.017" x 0.025", and 0.021" x 0.025").

When comparing the effect of the wire material, there were no statistically significant differences between any of the curves for the 0.016" x 0.022" CNA wires versus the 0.016" x 0.022" NiTi wires. This fact was also true regarding the curves for the 0.017" x 0.025" CNA wires versus the 0.017" x 0.025" NiTi wires. Thus, the material for these smaller dimension wires did not produce a statistically significant difference at either the incisor or the molar bracket. However, for the 0.021" x 0.025" wires, there was a statistically significant difference for the CNA versus NiTi curves for two of the force components at the incisor bracket (mesial/distal forces and facial/palatal forces). These p-values (< 0.05) showed that the entire curves were different for both

materials, and in both cases, the CNA wire delivered higher force magnitudes than the NiTi wire. Although there were no statistically significant differences shown for the entire curves for the other components, a careful examination showed a notable difference over a segment of some of the curves. Figure 26 shows two examples of this difference between 0.021" x 0.025" CNA and NiTi wires. This figure shows a graph of a force component and a graph of a moment component at one bracket, and in both graphs, the curves from each of the six wires for that specific component are plotted together.

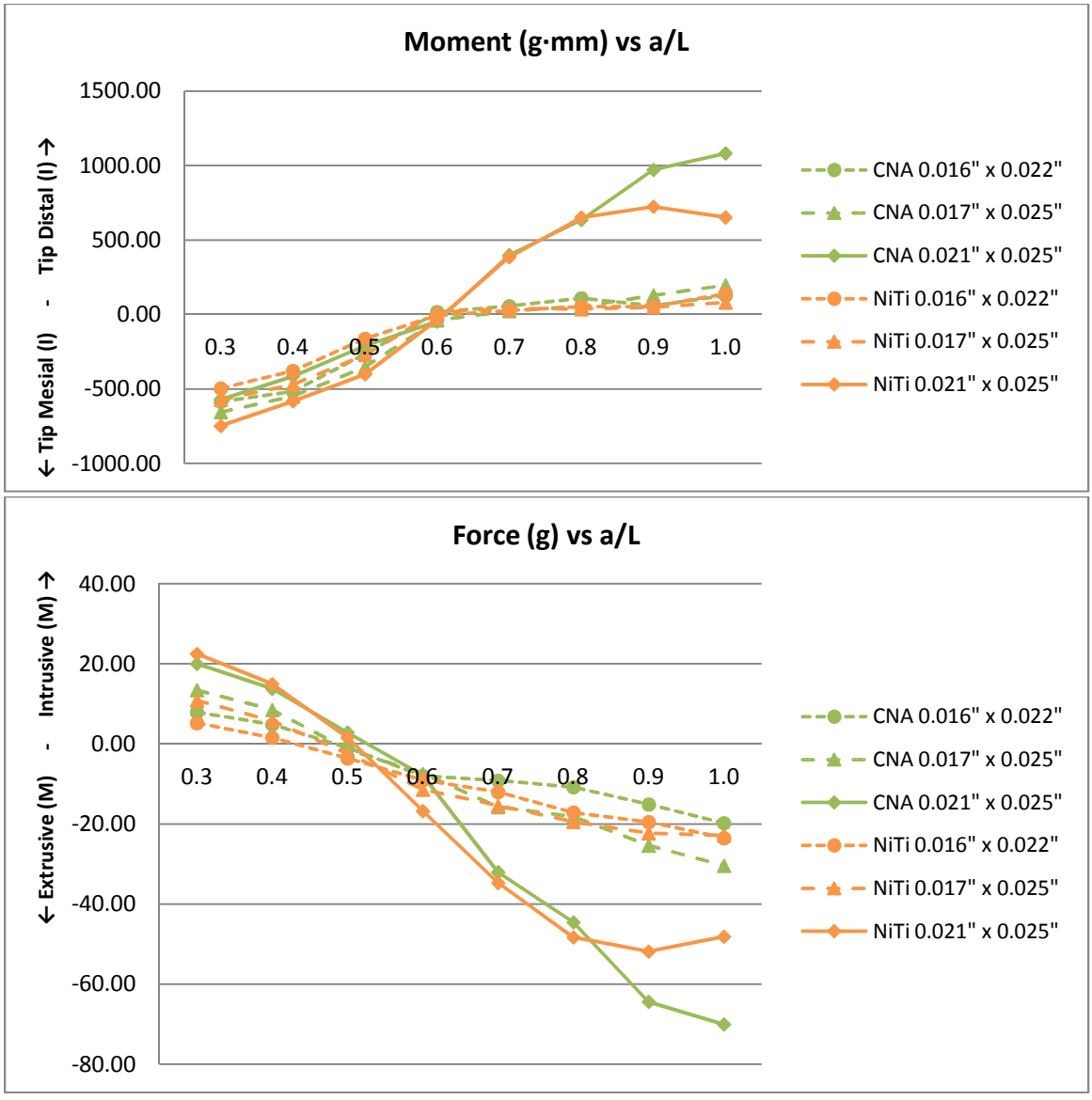

Figure 26

As previously mentioned, the smaller dimension wires for both materials showed very similar curves. In addition, the curves for the 0.021" x 0.025" CNA wire and the 0.021" x 0.025" NiTi wire were both similar for a/L = 0.3 – 0.8 in both examples. However, after a/L = 0.8, the CNA curves continued to increase in magnitude, while the NiTi curves appeared to become level. This phenomenon was likely due to the NiTi wires exhibiting their superelastic properties. When the bend was close to the molar, the deflection was great enough to produce SIM, and the NiTi wire entered the superelastic plateau region of its stress-strain curve. Conversely, the CNA wire continued to behave like an elastic wire as the deflection increased because the moment and force magnitudes also continued to increase. While comparing v-bends in straight segments of NiTi and TMA wires, Quick et al. observed the same superelastic pattern with the NiTi wires at greater deflections. (3)

In comparing the effect of the wire dimensions, there were no statistically significant differences between any of the curves for the 0.016" x 0.022" wires versus the 0.017" x 0.025" wires. This was true at both the incisor and molar brackets for both the CNA and NiTi wires. However, there were statistically significant differences at certain components when comparing the 0.021" x 0.025" wires to either the 0.016" x 0.022" wires or the 0.017" x 0.025" wires. This was true at both the incisor and molar brackets for both the CNA and NiTi wires. In general, the 0.021" x 0.025" wires delivered forces and moments with higher magnitudes than either of the smaller dimension wires. This effect could be expected because 0.021" x 0.025" wires have a much greater cross-sectional area than either of the other two wires, which are more similar. When comparing two wires of the same material, the springiness (inverse of the stiffness)

decreases by a power of four to the ratio of the cross-sectional areas of the larger wire versus the smaller wire. (24) Consequently, a small increase in the wire dimensions can have a large effect on the springiness and, therefore, the amount of force delivered. In addition, there is a much lower degree of play in the 0.021" x 0.025" wires in all three dimensions compared to the smaller dimension wires. Thus, when using the 0.021" x 0.025" wires, more of the activation force is transferred to the brackets, which creates higher force and moment magnitudes.

Although there was much to be learned from the current study, additional future studies could add to the understanding of the 3D force systems created by orthodontic appliances. One drawback of the current study was that only two sensors were available, so the forces and moments could be measured at only two teeth. The addition of more sensors would allow the study of more complex force systems, such as those that include three or more brackets arranged in an arch. This would be particularly useful clinically as orthodontists more commonly engage more than just the first molars and incisors in an arch wire. One more drawback was that wires with bends at a/L = 0.2 and less were not available to test. Including these wires could have provided a more thorough understanding of the effects caused by varying the position of the bends. In order to make a study directly comparable to the original 2D data described by Burstone et al., it would be worthwhile to reproduce the conditions they used for their mathematical calculations in an in vitro study. Although these experiments would involve a 2D setup (two aligned brackets in one plane), they would more easily highlight the differences between the computer simulations and in vitro experiments as well as add the moments and forces in the other planes, which were not reported previously.

Another potential drawback of this study was that it did not simulate the oral environment. Factors such as temperature, saliva, occlusion, and several others could affect the force systems produced. Of those factors mentioned above, temperature is one that can be easily simulated in a laboratory environment. In a clinical study, Moore et al. found that the intraoral temperature remained within the 33 ºC – 37 ºC range for 79% of the time, higher temperatures were experienced for only 1% of the time, and cooler temperatures for 20% of the time. The most frequent temperatures were between 35 ºC – 36 ºC, and therefore, the authors recommended that any in vitro testing of wires be performed at 35.5 ºC. (25) Tonner and Waters found that an increase in temperature resulted in a higher deactivation force plateau for NiTi wires. (26) Furthermore, Lim et al. conducted in vitro experiments to determine the effect of temperature on T-loops made of NiTi and TMA. The results showed that between 10 ºC – 50 ºC, NiTi wires produced higher force and moment values with increasing temperatures, but the M:F ratio remained relatively constant. For the TMA T-loops, temperature had minimal influence on the forces, moments, and M:F ratios. (27) In the current study, the temperature was maintained at room temperature (22.5 ºC ± 0.5 ºC). Conducting the experiments at a higher temperature to simulate intraoral temperature may have produced different results, especially for the NiTi wires. Nonetheless, the current study still provided a strong foundation of knowledge regarding the complete 3D force systems produced by vertical v-bends in a curved arch wire when engaged in a 2x2 orthodontic appliance setup.

Conclusions:

1. Although a v-bend is placed in an arch wire commonly to take advantage of the vertical forces and/or moments in the sagittal plane, forces and moments exist in all three planes of space, which have the ability to cause unwanted side effects.
2. Varying the position of the v-bend within the interbracket distance between the central incisor and first molar changed the force system in distinct patterns for each of the force and moment components.
3. When comparing the different wire materials, CNA and NiTi wires produced similar force systems in the 0.016" x 0.022" and 0.017" x 0.025" wires. For the 0.021" x 0.025" wires, the CNA wires tended to create forces and moments with higher magnitudes. In addition, the 0.021" x 0.025" NiTi wires appeared to exhibit their superelastic properties at higher deflections.
4. When comparing the wires of different dimensions for both CNA and NiTi, the 0.016" x 0.022" and 0.017" x 0.025" wires produced similar force systems, while the 0.021" x 0.025" wires produced forces and moments of greater magnitudes.

Appendix:

Figures 27 – 38 show a series of graphs displaying the magnitude and direction of a particular force or moment component versus the a/L ratio in relation to the global coordinate system. The graphs are grouped by the wire type (material and dimensions). The vertical axes are labeled with the direction of tooth movement above and below the horizontal axis. In cases where the descriptions differ for the incisor bracket and molar bracket, they are labeled with (I) or (M), respectively. The horizontal axes are labeled with the a/L ratio.

Figure 27: Force components, NiTi 0.016" x 0.022"

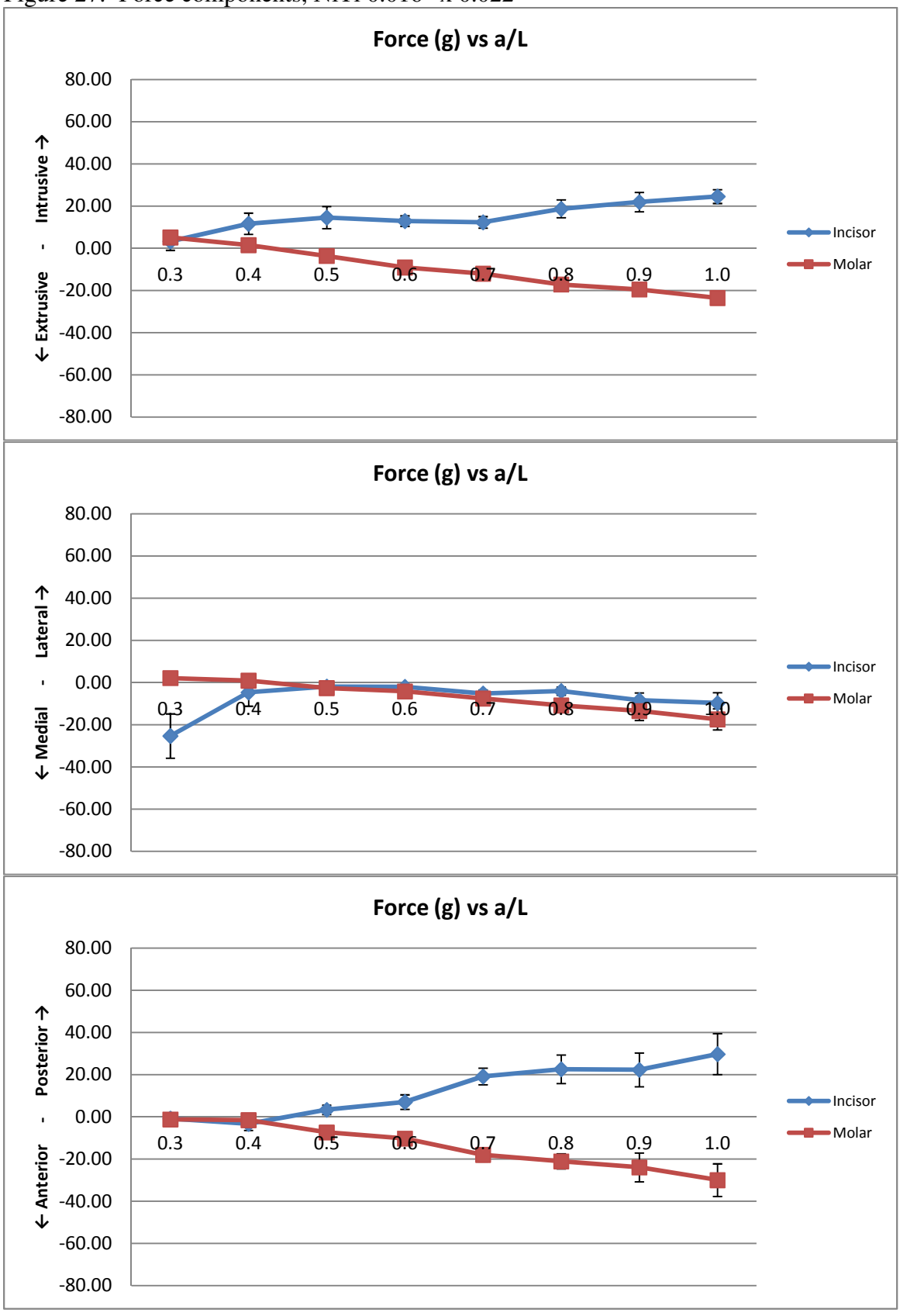

Figure 28: Moment components, NiTi 0.016" x 0.022"

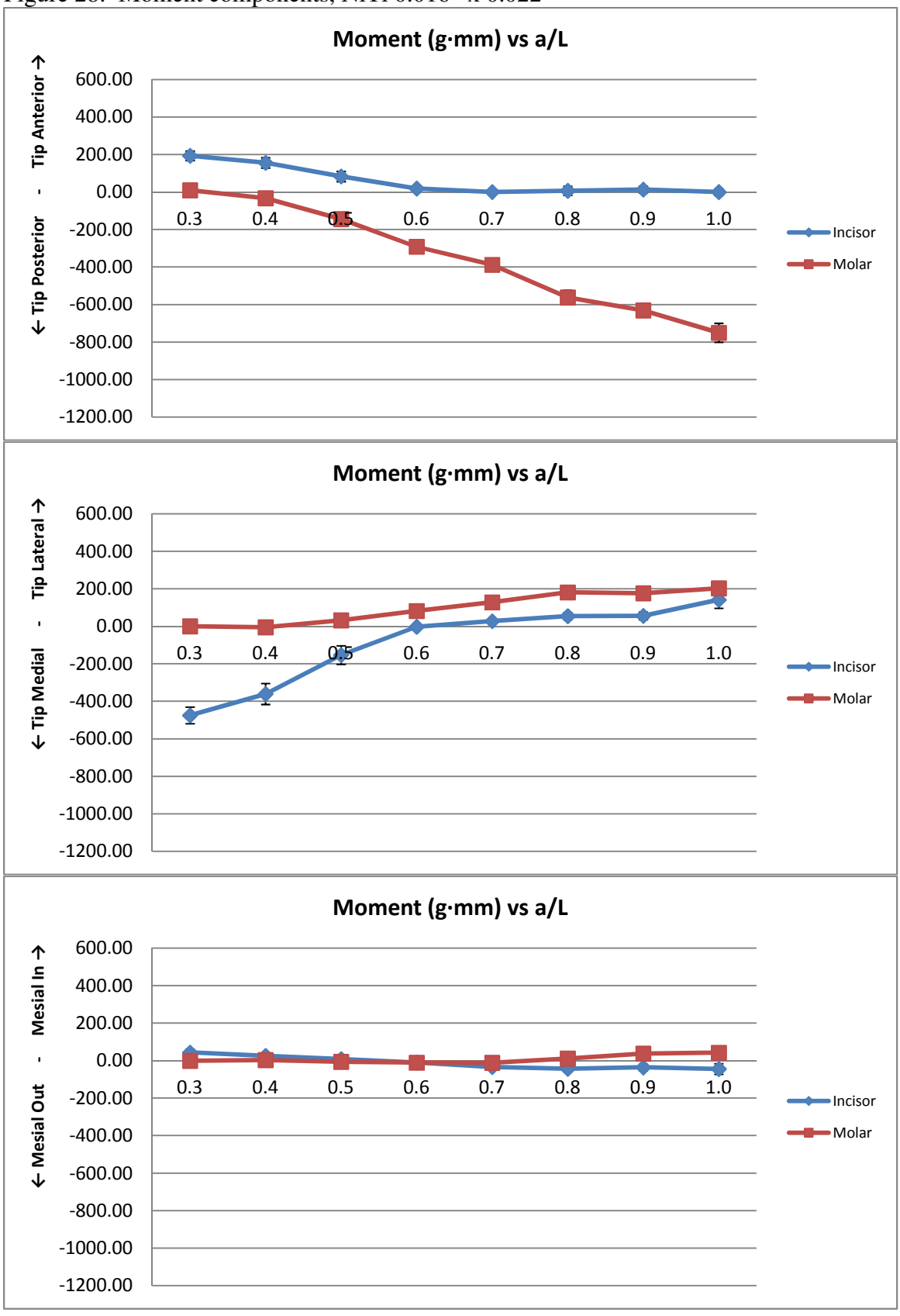

Figure 29: Force components, NiTi 0.017" x 0.025"

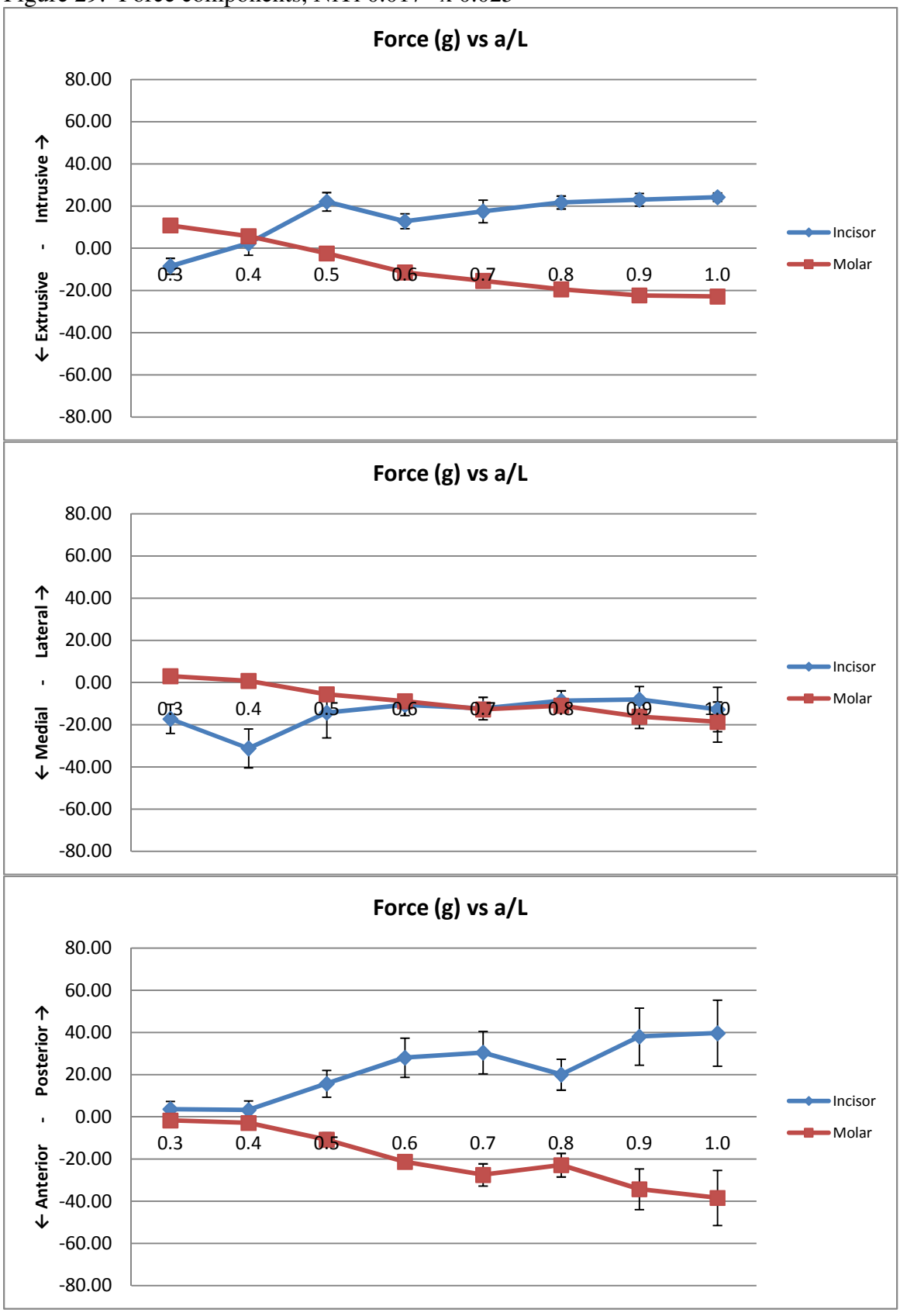

Figure 30: Moment components, NiTi 0.017" x 0.025"

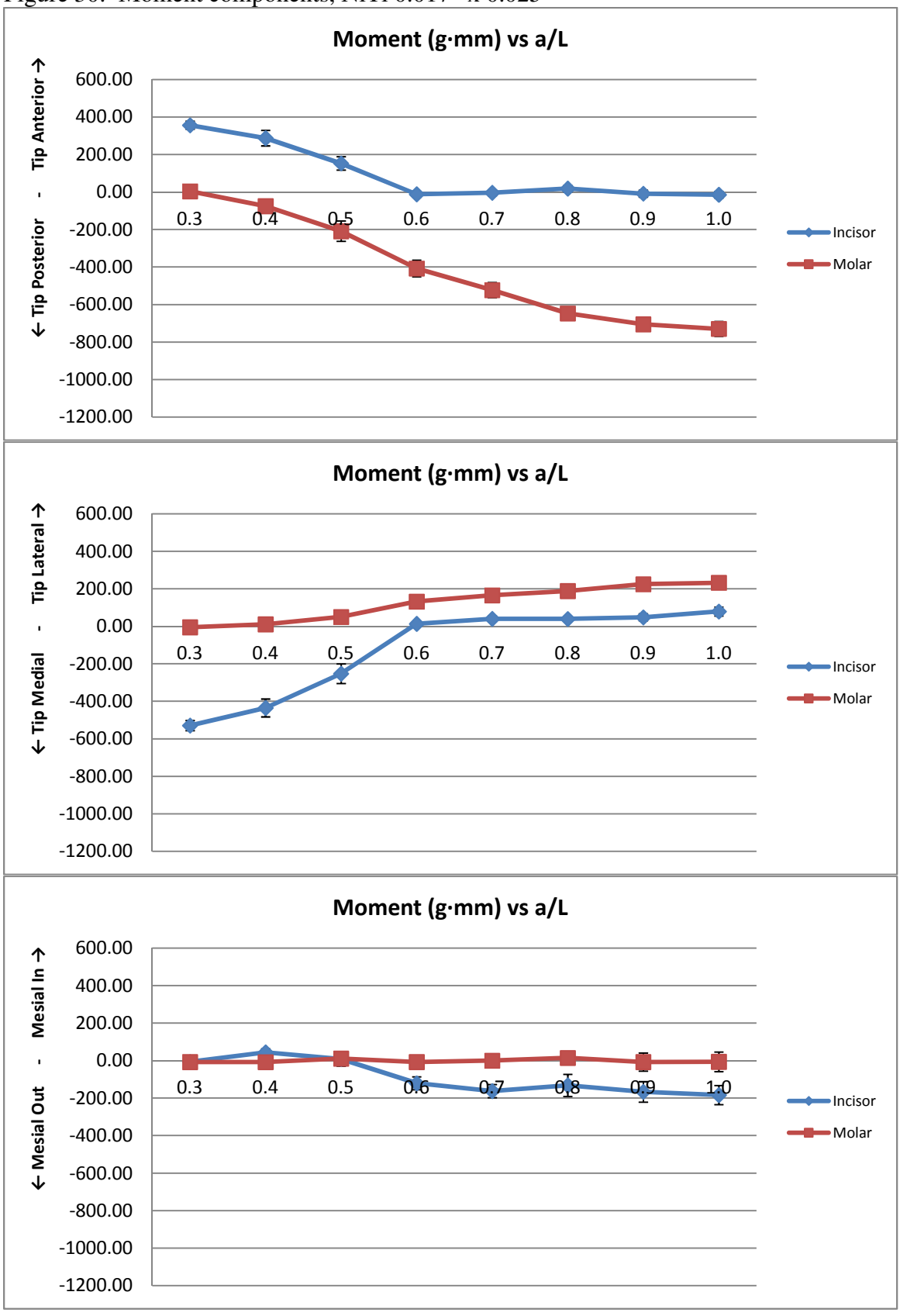

Figure 31: Force components, NiTi 0.021" x 0.025"

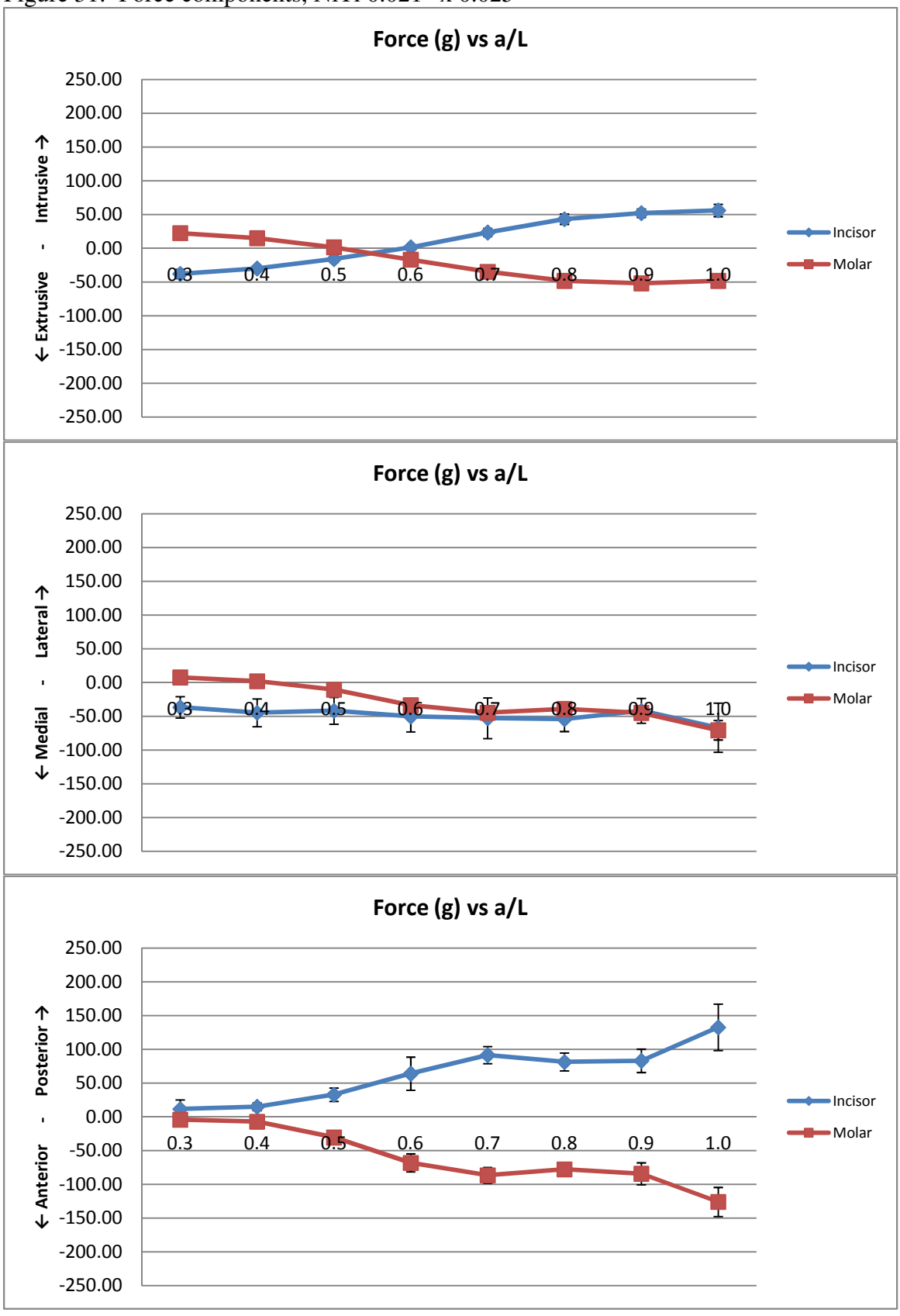

Figure 32: Moment components, NiTi 0.021" x 0.025"

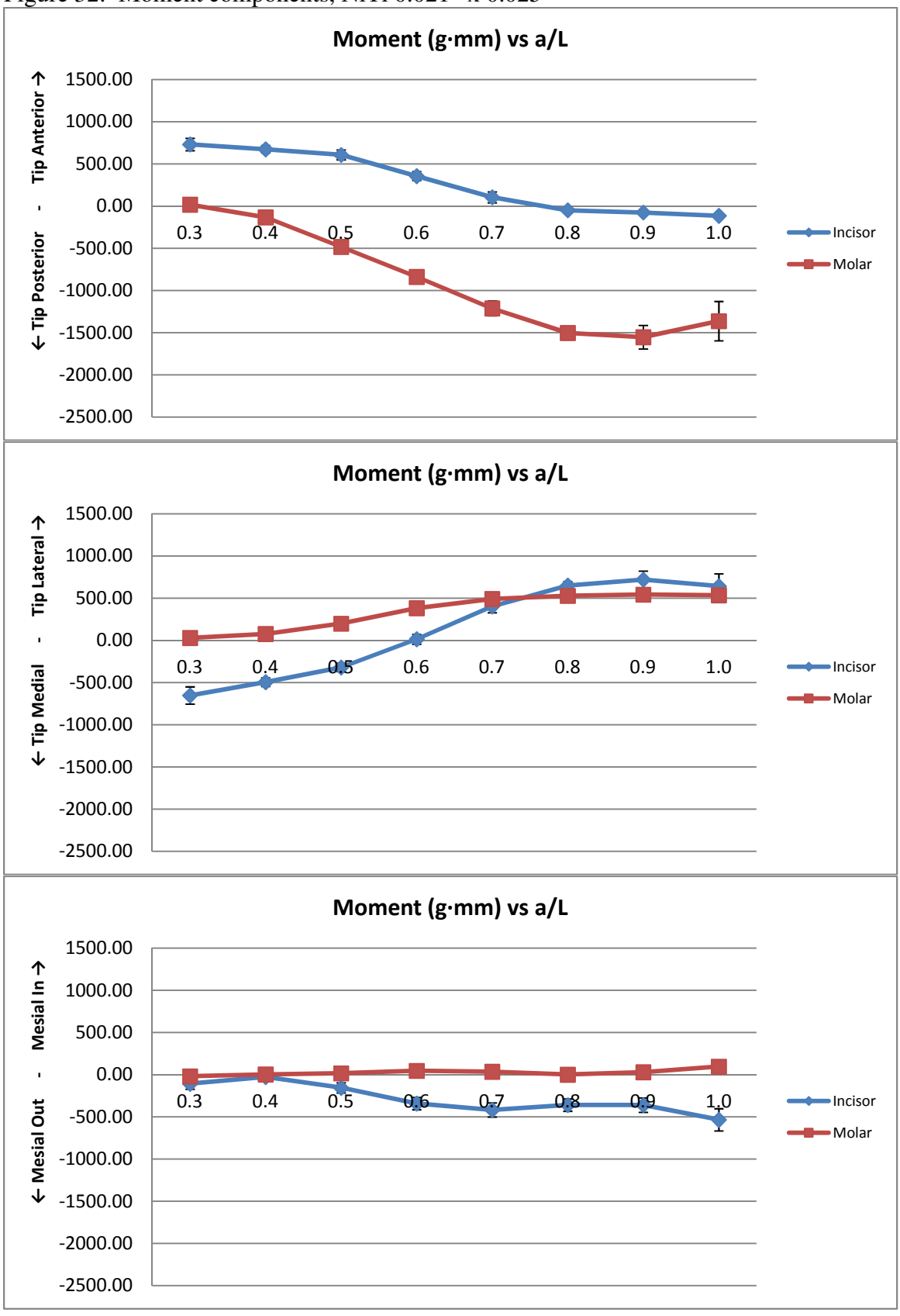

Figure 33: Force components, CNA 0.016" x 0.022"

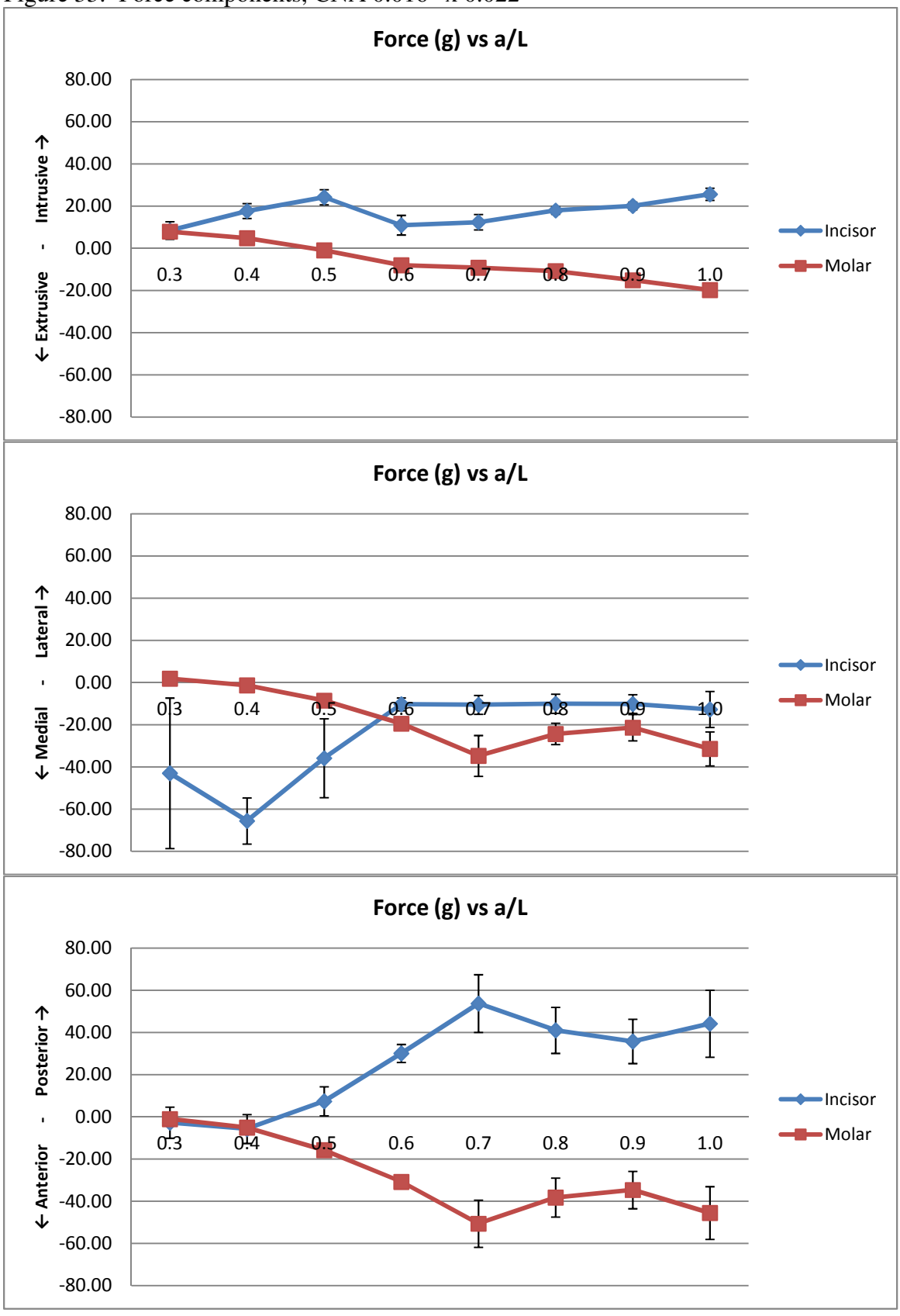

Figure 34: Moment components, CNA 0.016" x 0.022"

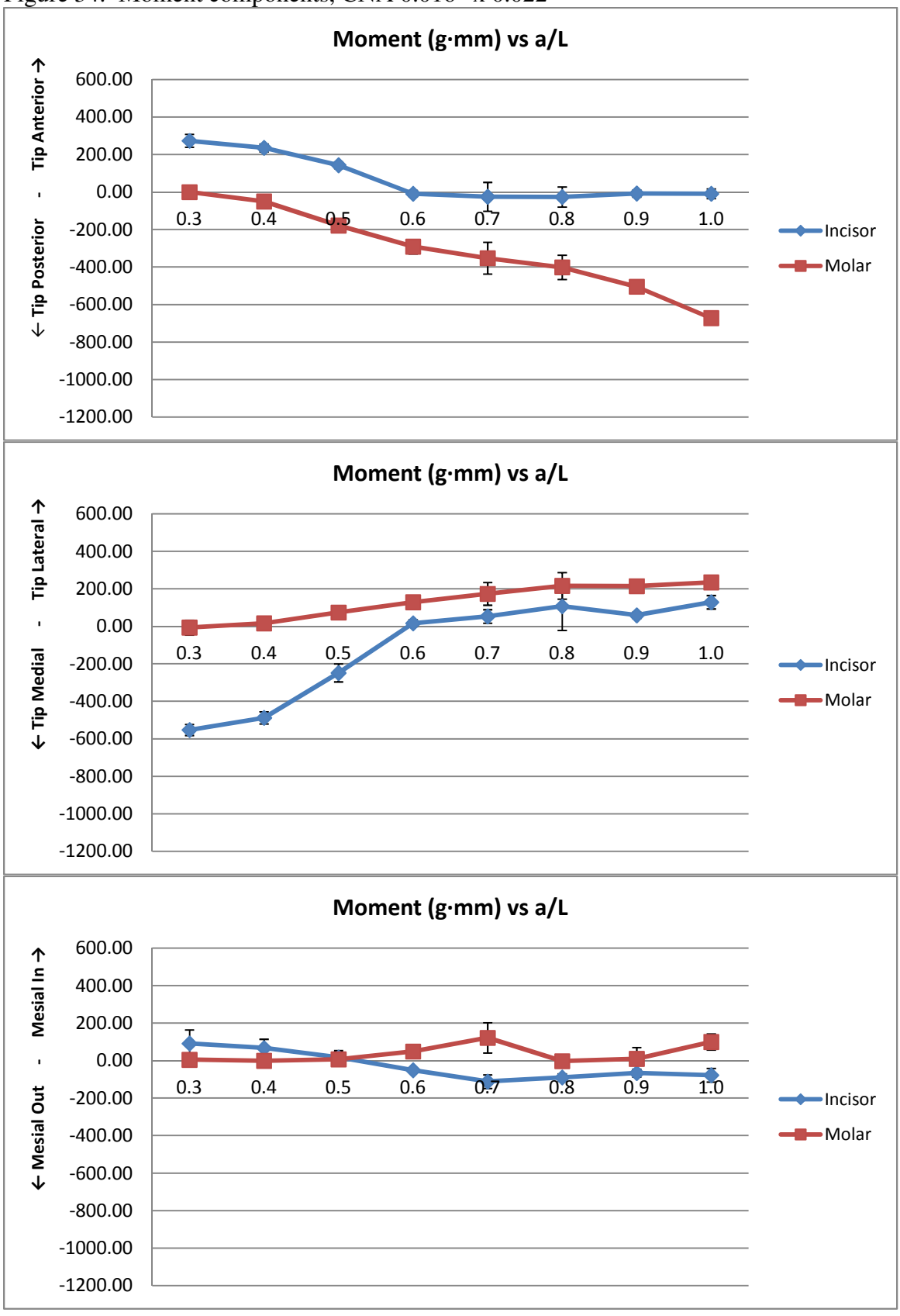

Figure 35: Force components, CNA 0.017" x 0.025"

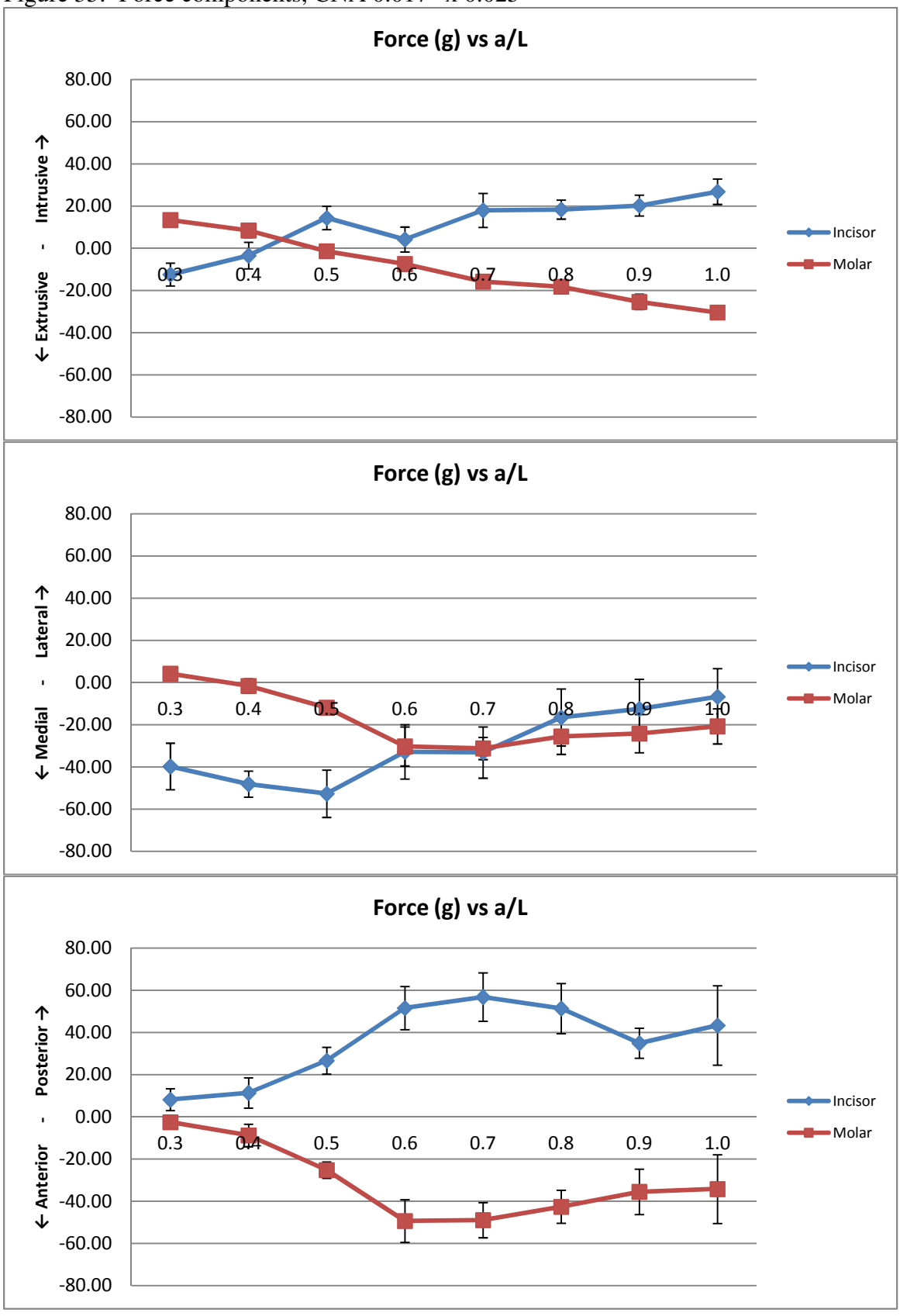

Figure 36: Moment components, CNA 0.017" x 0.025"

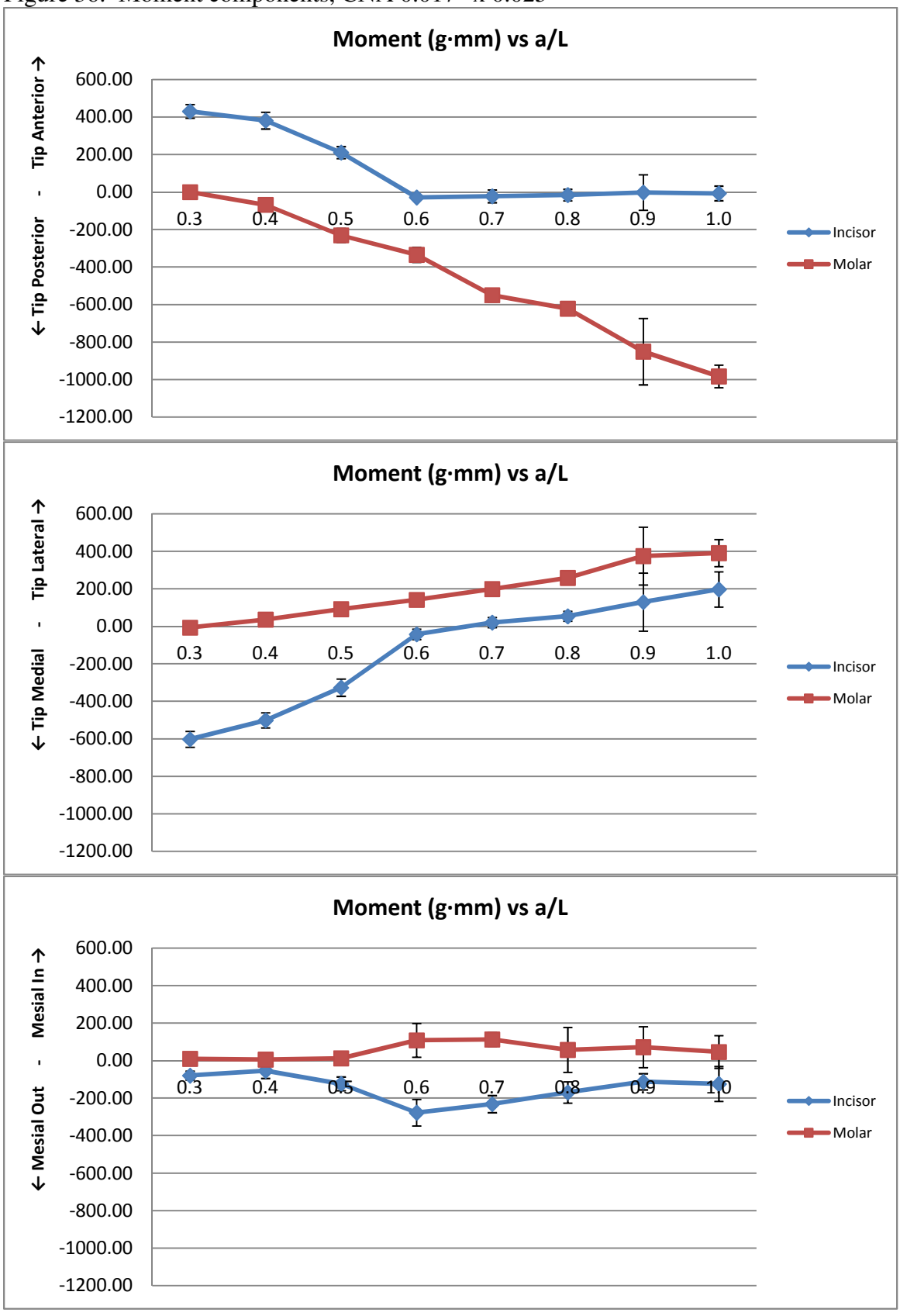

Figure 37: Force components, CNA 0.021" x 0.025"

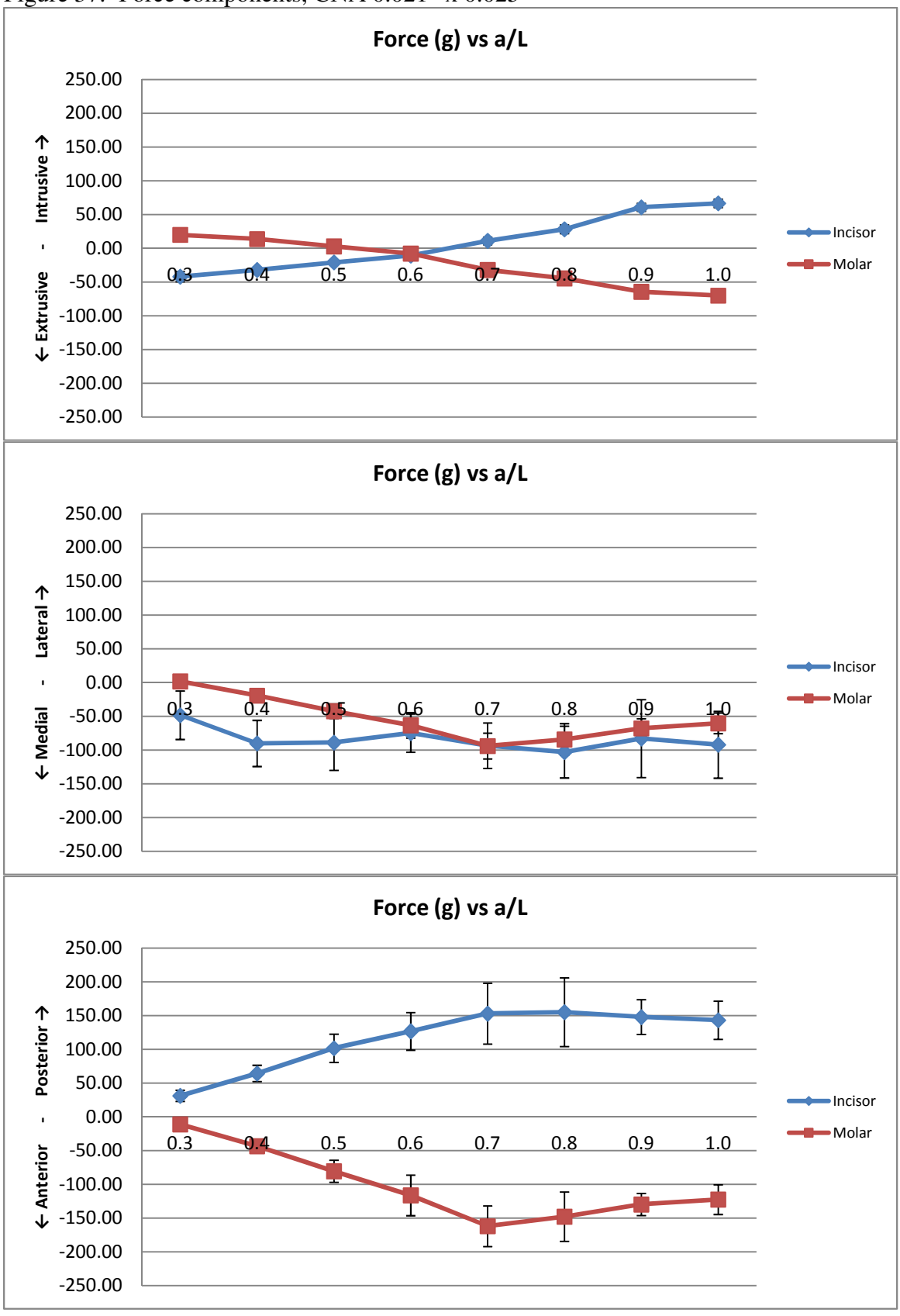

Figure 38: Moment components, CNA 0.021" x 0.025"

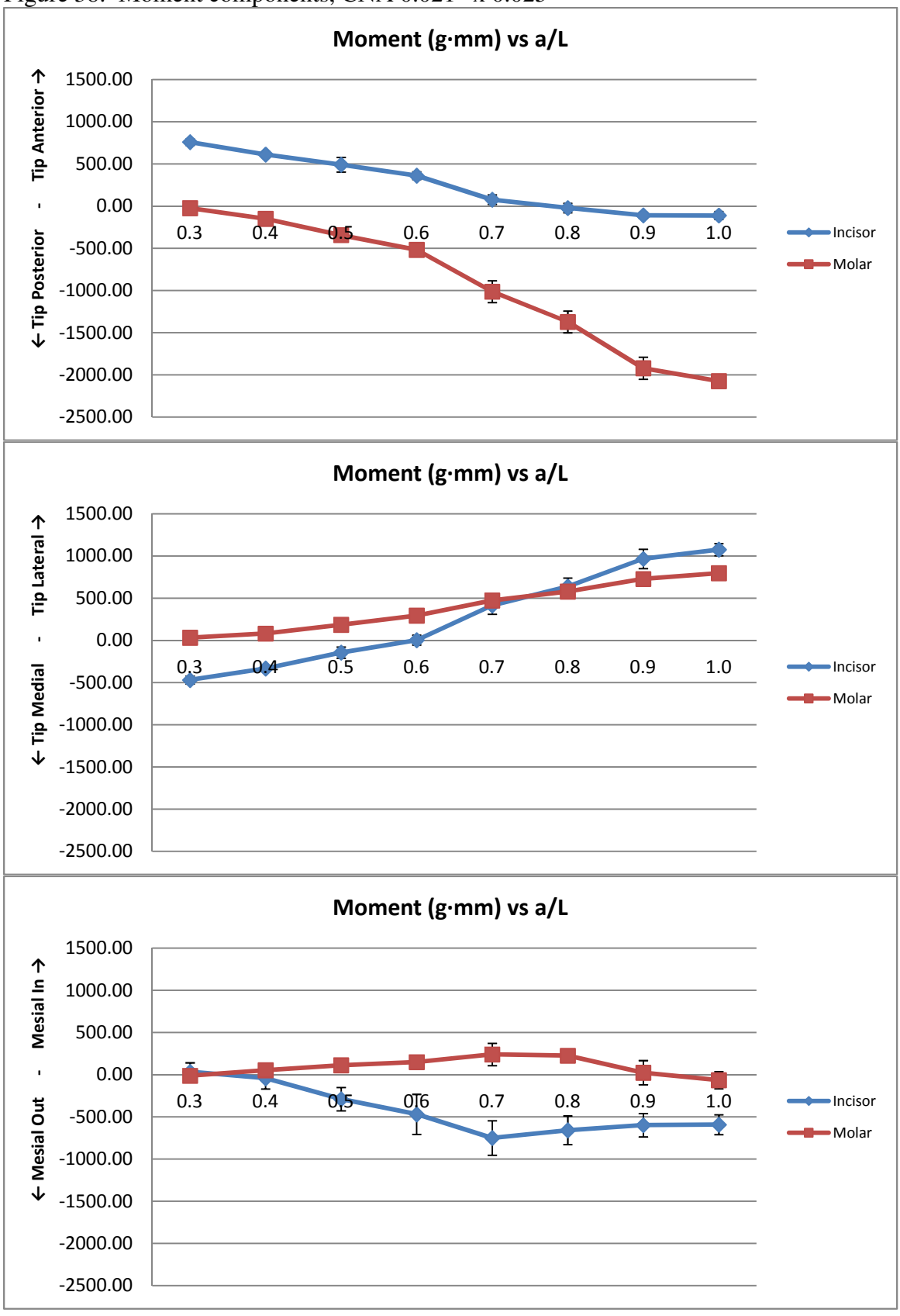

References:

1. Burstone, C J and Koenig, H A. Force Systems from an Ideal Arch. *American Journal of Orthodontics.* March 1974, Vol. 65, 3, pp. 270-289.
2. Burstone, C J and Koenig, H A. Creative Wire Bending - The Force System from Step and V Bends. *American Journal of Orthodontics and Dentofacial Orthopedics.* 59-67, January 1988, Vol. 93, 1.
3. Quick, A N, Lim, Y, Loke, C, Juan, J, Swain, M, and Herbison, P. Moments Generated by Simple V-Bends in Nickel Titanium Wires. *The European Journal of Orthodontics.* August 2011, Vol. 33, 4, pp. 457-460.
4. Isaacson, R J, Lindauer, S J and Conley, P. Responses of 3-Dimensional Arch Wires to Vertical V-Bends: Comparisons with Existing 2-Dimensional Data in the Lateral View. *Seminars in Orthodontics.* March 1995, Vol. 1, 1, pp. 57-63.
5. Kuhlberg, A and Nanda, R. Principles of Biomechanics. [book auth.] Ravindra Nanda. *Biomechanics and Esthetic Strategies in Clinical Orthodontics.* St. Louis : Elsevier Inc., 2005, pp. 1-16.
6. Nanda, R and Kuhlberg, A. Principles of Biomechanics. [book auth.] Ravindra Nanda. *Biomechanics in Clinical Orthodontics.* Philadelphia : Saunders, 1997.
7. Smith, R J and Burstone, C J. Mechanics of Tooth Movement. *American Journal of Orthodontics.* April 1984, Vol. 85, 4, pp. 294-307.
8. Ronay, F, Kleinert, W, Melsen, B, and Burstone, C J. Force System Developed by V Bends in an Elastic Orthodontic Wire. *American Journal of Orthodontics and Dentofacial Orthopedics.* October 1989, Vol. 96, 4, pp. 295-301.
9. Santoro, M, Nicolay, O F and Cangialosi, T J. Pseudoelasticity and thermoelasticity of nickel-titanium alloys: A clinically oriented review. Part I: Temperature transitional ranges. *American Journal of Orthodontics and Dentofacial Orthopedics.* June 2001, Vol. 119, 6, pp. 587-93.
10. Ulitmate Wireforms, Inc. *Wires.* [Powerpoint Presentation] Bristol, CT : s.n., 2006.
11. Santoro, M, Nicolay, O F and Cangialosi, T J. Pseudoelasticity and thermoelasticity of nickel-titanium alloys: A clinically oriented review. Part II: Deactivation forces. *American Journal of Orthodontics and Dentofacial Orthopedics.* June 2001, Vol. 119, 6, pp. 594-603.
12. Burstone, C J and Goldberg, A J. Beta titanium: A new orthodontic alloy. *American Journal of Orthodontics.* February 1980, Vol. 77, 2, pp. 121-132.
13. Johnson, E. Relative Stiffness of Beta Titanium Archwires. *Angle Orthodontist.* 2003, Vol. 73, 3, pp. 259-269.
14. Kusy, R P. A Review of Contemporary Archwires: Their Properties and Characteristics. *Angle Orthodontist.* 1997, Vol. 67, 3, pp. 197-208.

15. Kapila, S and Sachdeva, R. Mechanical Properties and Clinical Applications of Orthodontic Wires. *American Journal of Orthodontics and Dentofacial Orthopedics.* August, 1989, Vol. 96, 2, pp. 100-109.

16. Ultimate Wireforms, Inc. Ultimate Wireforms, Inc. *Relational Forces.* [Online] 2010. http://www.ultimatewireforms.com/support-material-selection.php#relationalforces.

17. Kusy, R P, Whitley, J Q and Gurgel, J. Comparisons of surface roughnesses and sliding resistances of 6 titanium-based or TMA-type archwires. *American Journal of Orthodontics and Dentofacial Orthopedics.* 2004, Vol. 126, 5, pp. 589-603.

18. Badawi, H M, Toogood, R W, Carey, J P, Heo, G, and Major, P W. Three-Dimensional Orthodontic Force Measurements. *American Journal of Orthodontics and Dentofacial Orthopedics.* October 2009, Vol. 136, 4, pp. 518-528.

19. Chen, J, Isikbay, S C and Brizedine, E J. Quantification of three-dimensional orthodontic force systems of T-loop archwires. *Angle Orthodontist.* 2010, Vol. 80, 4, pp. 754-758.

20. Fok, J, Toogood, R W, Badawi, H, Carey, J P, and Major, P W. Analysis of maxillary arch force/couple systems for a simulated high canine malocclusion Part 1. Passive ligation. *Angle Orthodontist.* July 20, 2011, Vol. Epub ahead of print.

21. Fok, J, Toogood, R W, Badawi, H, Carey, J P, and Major, P W. Analysis of maxillary arch force/couple systems for a simulated high canine malocclusion Part 2. Elastic ligation. *Angle Orthodontist.* June 14, 2011, Vol. Epub ahead of print.

22. Joch, A, Pichelmayer, M and Weiland, F. Bracket slot and archwire dimensions: manufacturing precision and third order clearance. *Journal of Orthodontics.* 2010, Vol. 37, pp. 241-249.

23. Isaacson, R J and Rebellato, J. Two-Couple Orthodontic Appliance Systems: Torquing Arches. *Seminars in Orthodontics.* 1995, Vol. 1, 1, pp. 31-36.

24. Proffit, W R. Mechanical Principles in Orthodontic Force Control. [book auth.] William R. Proffit, Henry W. Fields and David M. Sarver. *Contemporary Orthodontics.* 4th. St. Louis : Mosby Elsevier, 2007, p. 369.

25. Moore, R J, Watts, J T, Hood, J A, and Burritt, D J. Intra-oral Temperature Variation over 24 Hours. *European Journal of Orthodontics.* 1999, Vol. 21, pp. 249-261.

26. Tonner, R I and Waters, N E. The characteristics of super-elastic Ni-Ti wires in three-point bending. Part I: The effect of temperature. *European Journal of Orthodontics.* 1994, Vol. 16, 5, pp. 409-19.

27. Lim, Y, Quick, A, Swain, M, and Herbison, P. Temperature Effects on the Forces, Moments and Moment to Force Ratio of Nickel-Titanium and TMA Symmetrical T-loops. *Angle Orthodontist.* 2008, Vol. 78, 6, pp. 1035-42.

28. Laino, G, De Santis, R, Gloria, A, Russo, T, Quintanilla, D S, Laino, A, et al. Calorimetric and Thermomechanical Properties of Titanium-Based Orthodontic Wires: DSC–DMA Relationship to Predict the Elastic Modulus. *Journal of Biomaterials Applications.* Feb 22, 2011, Vol. Epub ahead of print.